Doctor of Philosophy

Role of type 4 sphingosine-1-phosphate receptor in genesis of non-alcoholic steatohepatitis

The Graduate School

of the University of Ulsan

Department of Medical Science

Chung Hwan Hong

Role of type 4 sphingosine-1-phosphate receptor in genesis of non-alcoholic steatohepatitis

Supervisor: Eun Hee Koh

A Dissertation

Submitted to

The Graduate School of the University of Ulsan

In partial Fulfillment of the Requirements

for the Degree of

Doctor of Philosophy

by

Chung Hwan Hong

Department of Medical Science

University of Ulsan, Korea

February, 2022

Role of type 4 sphingosine-1-phosphate receptor in genesis of non-alcoholic steatohepatitis

This certifies that the dissertation of Chung Hwan Hong is approved.

Beom Jun Kim *(Signature)*
(Chairman of Committee)

Eun Hee Koh *(Signature)*
(Committeeman)

Won Gu Kim *(Signature)*
(Committeeman)

Jonggi Choi *(Signature)*
(Committeeman)

Seung Eun Lee *(Signature)*
(Committeeman)

Department of Medical Science

University of Ulsan, Korea

February 2022

CONTENTS

ABSTRACT

NLRP3 inflammasome activation is important in the pathogenesis of non-alcoholic steatohepatitis (NASH). Here we show that genetic depletion of S1PR4 protected mice from N ASH development. Genetic depletion of *S1pr4* also protected the mice against hepatic inflamma tion and fibrosis. *S1pr4* depletion in hepatic macrophages inhibited lipopolysaccharide-mediated Ca^{++} release and deactivated the NLR Family pyrin domain containing 3 (NLRP3) inflammasome. S1P increased the expression of *S1pr4* in hepatic macrophages and activated NLRP3 inflamma some through phospholipase C/inositol triphosphate (IP_3) /IP_3 receptor-dependent [Ca^{++}] signali ng. Administration of a novel sphingolipid SLB736 prevents development of NASH in mice by inhibiting NLRP3 inflammasome in Kupffer cells. SLB736 acted as a selective functional antagonist of S1PR4, and did not induce lymphopenia. S1PR4 may become a new therapeutic target of NASH.

Keywords: hepatic macrophages, NLRP3 inflammasome, S1P, Ca^{++}

Lists of figures

Introduction

Nonalcoholic fatty liver disease (NAFLD) has become a major challenge to healthcare systems worldwide. NAFLD is an umbrella term that comprises a continuum of liver conditions varying in severity of injury and resulting fibrosis. Between 10 and 20% of patients with NAFLD develop non-alcoholic steatohepatitis (NASH), which can progress to liver cirrhosis and hepatocellular carcinoma. NASH is defined as a more serious process with inflammation and hepatocyte damage (steatohepatitis); typically, NASH is accompanied by percicellular fibrosis, which may progress to cirrhosis. Although NAFLD or NASH can be strongly suspected in an individual on the basis of imaging and clinical features (such as the presence of metabolic comorbidities and abnormal lab tests), NASH can only be definitely diagnosed by liver biopsy; additional subgroups of NASH have also been defined recently[1]. Although there has been steady progress in clarifying the pathogenesis of NAFLD, identifying therapeutic targets and advancing drug development, there are significant unmet challenges, and no agent is approved yet for this condition.[2-4]

The inflammasome was described a decade ago as a large intracellular signaling platform that contains a cytosolic pattern recognition receptor, especially a nucleotide-binding oligomerization domain-like receptor (NLR) or an absent in melanoma 2 (AIM2)-like receptor. Among NLR inflammasome complexes, the NLRP3 inflammasome has been the most widely characterized and is a crucial signaling node that controls the maturation of two proinflammatory interleukin (IL)-1 family cytokines: IL-1β and IL-18. Activation of the pattern recognition receptor NLRP3 leads to recruitment of the adapter apoptosis-associated speck-like protein containing a C-terminal caspase recruitment domain (ASC), resulting in the activation of pro-caspase-1 into its cleaved form[5-8]. Caspase-1 is known as an inflammatory caspase that plays a role in the maturation of IL-1β and IL-18 into active cytokines and the initiation of pyroptosis by autocatalysis and activation.[9-12] Activation of the NLRP3 inflammasome is thought be regulated at both the transcriptional and post-translational levels. The first signal in inflammasome activation involves the priming signal, induced by the toll-like receptor (TLR)/nuclear factor (NF)-κB pathway, to upregulate the expression of NLRP3, the level of which is otherwise relatively low in numerous cell types. Signal 2 is transduced by various PAMPs and DAMPs to activate the functional NLRP3 inflammasome by initiating assembly of a multi-protein complex consisting of NLRP3, the adaptor protein ASC, and pro-caspase-1. Several molecular mechanisms have been suggested for NLRP3 activation to induce caspase-1 activation and IL-1β maturation. These include pore formation and potassium (K+) efflux, lysosomal destabilization and rupture, and mitochondrial reactive oxygen species generation[10,13,14]. NLRP3 inflammasome activators are chemically and structurally distinct from each other and/or known to engage the cell in disparate ways. For example, extracellular ATP signals through the cell surface P2X7 receptor (P2X7R), nigericin is a bacterial toxin with potassium ionophore activity, and crystal formation is necessary for several stimuli to activate the NLRP3 inflammasome (e.g., uric acid, silica). Therefore, it is generally believed that these stimuli engage the NLRP3 inflammasome indirectly, by triggering some signal associated with cellular stress that can be recognized by the complex.

Inflammasome activation in liver macrophages is also an important contributor to liver inflammation and fibrosis. Macrophages are key players of the innate immune system and in the liver comprise liver-resident Kupffer cells and recruited monocyte-derived macrophages. Kupffer cell depletion also leads to decreased expression of inflammatory cytokines, attenuated inflammation and liver cell death (necroinflammation), as well as oxidative damage and expression of fibrosis-related genes. In addition to liver-resident Kupffer cells, monocyte-derived macrophages have a major role in the pathogenesis

of NAFLD and NASH. The monocyte flux to the liver is primarily regulated by the chemokine CCL2, which is produced by a number of cells but mostly monocytes or macrophages, and its cognate receptor, CCR2, which is expressed prominently by monocytes. Macrophages can be activated by various stimuli such as endotoxins, fatty acids, cholesterol and their metabolites, as well as molecules associated with hepatocyte damage[15-21].

Sphingosine-1-phosphate (S1P) is a membrane-derived lysophospholipid that acts primarily as an extracellular signaling molecule by activating five G protein-coupled receptors (S1PR1-5)[22]. S1P levels are mainly regulated by the relative complement of enzyme activities in a cell's sphingolipid metabolic pathway. In most tissues, including lymphoid tissue, S1P levels are extremely low[23,24]. Notable exceptions are the blood, where S1P levels are in the low-micromolar range and are mainly contributed by erythrocytes, and the lymph, where S1P levels are in the hundred-nanomolar range. Studies indicate that the producers of S1P, SPHK1 and SPHK2, are involved in the homeostasis of circulating S1P levels. More specifically, deletion of the genes that encode both kinases is embryonic lethal and results in embryos lacking S1P. Furthermore, conditionally knocking out these genes renders mice deficient in circulating S1P[23,25]. S1P signalling has a role in both the homing of immune cells to lymphoid organs and in controlling their egress into blood and lymph, an area that has received much recent attention. An important determinant driving egress is the S1P gradient that exists between tissues (which have low S1P levels) and vascular compartments (which have high S1P levels). The many diverse roles of S1P in innate and adaptive immunity, including immunosurveillance, immune cell trafficking and differentiation, immune responses and endothelial barrier integrity are mediated by its binding to one of five G-protein-coupled receptors, named S1PR1– S1PR5. Much less is known about the intracellular targets of S1P. Within the past decade, new intracellular targets of S1P have been characterized. S1P formed by SphK1 in response to TNF or interleukin-1 (IL-1) binds to TNF receptor-associated factor 2 (TRAF2) and cellular inhibitor of apoptosis 2 (cIAP2), respectively, and enhances their lysine-63-linked polyubiquitylation activities[26-28]. Receptor-mediated S1P signaling has become an attractive therapeutic target in several diseases such as chronic inflammatory disease, autoimmunity, cancer, and metabolic disease[29,30]. In the liver, S1PR2 participates in cholestasis-induced liver injury and in chronic liver injury induced by bile duct ligation, as well as in methionine-choline-deficient and high-fat diet, or carbon tetrachloride-mediated liver injury and fibrosis[31]. S1PR1 and S1PR3 are involved in HSCs motility and activation and play a crucial role in the angiogenic process required for fibrosis development[32,33]. The fundamental physiological role of the interaction between S1P and S1PRs in immune-cell function was recognized through studies of the immunosuppressant drug Fingolimod (codenamed FTY720). This compound rapidly induces lymphopaenia through the sequestration of lymphocytes in lymph nodes and by blocking the egress of mature thymocytes from the thymus. A breakthrough in the understanding of its mechanism, together with a link to S1PR signalling, came with the realization that FTY720 is a sphingosine analogue that could be phosphorylated by SPHKs to produce a S1PR ligand with potent effects, including S1PR agonism and the downregulation of S1PR expression. FTY720, a modulator of S1PRs, is used clinically as a drug to treat relapsing-remitting multiple sclerosis[34]. In addition, S1PRs have become attractive therapeutic targets in several other diseases, such as chronic inflammatory pathologies, autoimmunity, and cancer[35]. In particular, FTY720 was shown to prevent concanavalin A-induced liver injury[36-38], alcoholic liver disease[39] (ALD) and NASH[40].

In the present study, we found that administration of SLB736, a new chemical with sphingolipid structure, prevents the development of NASH and fibrosis by inhibiting NLRP3 inflammasome activation in Kupffer cells. We found that S1PR4 activation by S1P sequentially activated

phospholipase C and IP3 receptor in Kupffer cells to increase [Ca++] that activated NLRP3 inflammasome. SLB736 specifically bound to S1PR4, but internalized and degraded it to act as a functional antagonist of S1PR4. SLB736 decreased S1PR4 protein level in cultured macrophages and in the liver. S1PR4 heterozygous K/O ($S1PR4^{+/-}$) mice showed decreased NLRP3 inflammasome activation in Kupffer cells on high fat high cholesterol diet (HFHCD) feeding, and these mice were protected from NASH and hepatic fibrosis. Finally, administration of SLB736 did not induce lymphopenia, a well-known side effect of FTY720[41]. Taken together, functional antagonists of S1PR4 can become a novel strategy to prevent/ treat NASH and fibrosis.

Materials and Methods

Mice and diet

Mice were housed at ambient temperature (22 ± 1°C) with a 12:12 h light-dark cycle and free access to water and food. All animal use and experiment protocols were approved by the Institutional Animal Care and Use Committee of Asan Institute for Life Sciences, Seoul, Korea.

Eight-weeks-old male C57BL/6J mice were fed either normal chow diet (ND; 12% energy from fat), CDA + HFD containing 60 kcal fat and 0.1% methionine (A06071302, Research Diets, New Brunswick, NJ) for 6 weeks, MCDD (Dyets Inc., Bethlehem, PA) for 8 weeks, or HFHCD (60% energy from fat and 2.5% cholesterol, Dyets Inc.) for 12 weeks. In another group, mice were fed WD (TD.120330; 0.2% cholesterol + 22% hydrogenated vegetable oil, Envigo RMS, Inc., IN) supplemented with high fructose syrup in the drinking water for 16 weeks.56 After the indicated time of diet feeding, mice were fasted for 5 h in the morning before they were euthanized.

S1pr4+/- mice were purchased from Jackson Laboratories (mouse strains, 005799; Bar Harbor, ME). Eight-weeks-old male S1pr4+/- mice and their littermate control (S1pr4+/+) were fed either ND or HFHCD for 4 or 12 weeks. Considering the description in the MGI website (http://www.informatics.jax.org/marker/MGI:1333809) on the embryonic lethality of homozygous mutation of the S1PR4 gene, we used heterozygote mice for this study and observed the deletion of one copy of the S1PR4 gene.

Human liver samples

Human liver samples were obtained from liver explants of donors and recipients diagnosed with NASH undergoing liver transplantation at the Liver Transplantation Unit of the Hospital Clinic, Barcelona. Normal liver tissue was obtained from the surgical specimens of donor livers used for transplantation. A biopsy of the resected liver from the recipient was performed right after the hepatectomy and samples were fixed in formalin for histological examination. The protocol was approved by the Hospital Clinic/UB Ethics Committee (HCB/2012/8011) of Hospital Clinic, Barcelona, Spain.

Isolation and identification of hepatic macrophages

Hepatic macrophages were isolated from mice by collagenase digestion, gradient centrifugation, and selective adherence, [42] with modifications. Briefly, the mice were anesthetized and the peritoneal cavity was opened; the livers were perfused with Ca^{++} and Mg^{++}-free-Hank's balanced salt solution (LB 003-04, Welgene, Daegu, Korea) containing collagenase (17101-015, Gibco, Carlsbad, CA) and trypsin inhibitor (T2011, Sigma-Aldrich, St. Louis, MO). The digested livers were removed and placed in 60-mm petri dishes. The livers were frittered with forceps in RPMI1640 (LM 011-01, Welgene) supplemented with 10% (vol/vol) FBS (16000-044, Gibco). The cell suspensions were filtered through a sterile 100-μm nylon cell strainer (352360, Falcon) to remove undigested tissues and connective tissues. The cells were centrifuged for 5 min at 50 × g at room temperature to remove hepatocytes. The supernatants were transferred to clean 50 ml tubes. The supernatants were centrifuged at 1600 rpm (4°C) for 10 min, and the cell pellets were re-suspended in 20% OptiPrep and

gently layered on OptiPrep gradient (20, 11.5% and Hank's balanced salt solution) and centrifuged at 3000 rpm at 4°C for 17 min with the brake option off. Subsequently, the upper layers were removed and the cell fraction between 20% OptiPrep and 11.5% OptiPrep gradient were collected without contamination from the pellets. The collected layers were washed twice with RPMI1640 supplemented with 10% (vol/vol) FBS, and plated into 12-well or 24-well tissue culture plates. At 10 min after seeding, non-adherent cells (cell debris or blood cells) were removed by aspiration and fresh media were added. The next day, the cells were washed twice with 1 × PBS, and the attached hepatic macrophages were cultured for another 48 h, at which point they were ready for experimental use.

Hepatic macrophages were identified by flow cytometry using a monoclonal anti-F4/80 antibody. Briefly, after 48 h of culture, macrophages were detached by incubation with 0.25% trypsin for 5 min, and pelleted by centrifugation for 5 min at 100 rpm/min. The cells were then incubated with the anti-F4/80 antibody (clone BM8)-conjugated phycoerythrin (12-4801-82; Invitrogen, Carlsbad, CA) for 30 min at 4°C (1:200 dilution). The data were collected using the FACSCanto2 (BD Bioscience, San Jose, CA) and analyzed with the FlowJo software.

Bone marrow and spleen macrophage isolation

Bone marrow and spleen was excised and digested for 30 min with collagenase (Sigma) at 37 °C with shaking. Cell suspensions were filtered through a 70-μm sieve and centrifuged at 450 g for 5 min. Femurs were collected in RPMI. Bone marrow cells were flushed from the femurs and then depleted of RBCs using RBC lysis buffer (R7757, Sigma-Aldrich,). For macrophage staining, cells were incubated with FcBlock (101302, Biolegend, San Diego, CA) for 10 min in ice, then washed and stained with anti-F4/80 antibody (12-4801-82, Invitrogen) and anti-CD45.2 antibody (45-0454-82, Invitrogen) for 30 min on ice, in the dark. Macrophages were sorted as live CD45.2 and F4/80 double positive cells using a FACS Aria2 (BD Bioscience) into RPMI supplemented with 20% FBS.

Primary hepatocyte isolation and culture

Mice were perfused with Hank's balanced salt solution (Welgene) pre-warmed in a 42°C water bath. Then, 0.36 mg/ml collagenase (Gibco) and trypsin inhibitor (Sigma-Aldrich) were added immediately before liver perfusion as previously described[43].

Histological analysis

Liver tissue samples were fixed in 10% neutral buffered formalin and embedded in paraffin. Serial sections (5 μm-thick) were stained with hematoxylin and eosin, Masson's Trichrome, or Sirius Red, as appropriate.

Liver TG contents

TG content in the liver was determined in duplicate using the Sigma Triglyceride (GPO-Trinder) kit.

Real-time PCR analysis

Total RNA isolated from each sample was reverse-transcribed and the target cDNA levels were quantified by real-time PCR analysis using gene-specific primers. Total RNA was isolated using TRIzol (Invitrogen), and 1 μg of each sample was reverse-transcribed with random primers using the Reverse Aid M-MuLV Reverse Transcription Kit (Fermentas, Amherst, NY). The relative expression levels of each gene were normalized to that of 18S rRNA or *Tbp*.

Western blot analysis

Cell and liver samples were homogenized in lysis buffer (50 mM Tris, pH 7.4, 150 mM KCl, 4 mM EDTA, 4 mM EGTA and 1% NP-40 containing protease [04693132001, Roche, Carlsbad, CA, USA] and phosphatase [04906837001, Roche] inhibitor mixture tablets) at 4°C for 30 min. The resulting protein (40–50 μg) was subjected to immunoblotting with primary antibodies: antibodies against phosphorylated NF-kB and NF-kB were purchased from Cell Signaling (Danvers, MA). Anti-S1PR4 antibody was purchased from NOVUS (Centennial, CO). β-actin (A5441, Sigma-Aldrich) was used as housekeeping control. The signal intensities of protein bands were quantified with the ImageJ software (NIH, Bethesda, MD) and normalized using the intensity of the loading control.

IL-1β measurement

Mouse IL-1β in cell culture supernatants were measured using the mouse IL-1β /IL-1F2 Quantikine ELISA kit (DY401, R&D Systems, Minneapolis, MN).

Lentiviral-silencing S1pr4

The shRNA sequence for *S1pr4* was Forward: 5′-GCCTGCTGAACATCACACTGATCAAGAGTCAGTGTGATGTTCAGCAGGCTTTTTTG-3′; Reverse: 5′-CAAAAAAGCCTGCTGAACATCACACTGACTCTTGATCAGTGTGATGTTCAGCAGGC-3′. *S1pr4* shRNA were subcloned into the pCDH-MCS lentiviral vector (CD513B-1, System Biosciences, Mountain View, CA,), and the plasmids were transfected in Lenti-X 293T cells (632180, Clontech, Mountain View, CA) along with packaging plasmids pMDLg/pRRE (Addgene, 12251) and pRSV-Rev (12253, Addgene, Cambridge, MA) and enveloped plasmid pCMV-VSV-G (8454, Addgene) using Lipofectamine 3000 (L30000015, Invitrogen). Hepatic macrophages were infected with lentiviral vectors coding *S1pr4* shRNA for 12 hrs, at a range of multiplicity of infection (MOI) (0, 10, and 50). The medium was changed after 12 hrs.

Intracellular IP-one measurement

PLC activity was tested with the IP-one ELISA (72IP1PEA; Cisbio, Bedford, MA), in which hepatic macrophages were stimulated with LPS or S1P and then the cell culture medium was replaced with a fresh medium. Intracellular IP-one, a surrogate measure for the level of inositol triphosphate, was measured after treatment with LiCl (50 mM) to prevent the degradation of IP-one into myo-inositol.

The level of inositol triphosphate in cell lysates was measured using ELISA.

Calcium analysis by confocal microscopy

Hepatic macrophages were plated on 35 mm imaging dish (81156, Ibidi, Gräfelfing, Germany) at a density of 0.1×10^6 cells and incubated with Fluo-4/AM. Images of untreated cells were acquired at t = 0, and the cells were treated with 1 μg/ml LPS or 1 mM ATP in RPMI 1640. The cells were imaged for 5 min at 5 s intervals on a Zeiss LSM780 Confocal Imaging System using the 488 nm laser and emission in the range of 500–600 nm. The images were analyzed using Zen 2012 SP5 software by creating surfaces to encompass the volume of each cell. The absolute intensity for all cells in a field at different time points was obtained, and normalized to t=0 to calculate the fold increases in intensity. Data are displayed as the relative intensity of cells in a field.

Reagents for calcium signaling

BAPTA-AM (A1076, Sigma-Aldrich), U73122 (U6756, Sigma-Aldrich), 2-APB (D9754, Sigma-Aldrich), and Xes-c (X2628, Sigma-Aldrich) were used for detecting calcium signaling.

S1P treatment in hepatic macrophages

Hepatic macrophages were serum-starved for 6 h and then stimulated with 1 μM S1P (S9666, Sigma-Aldrich) for 2 h.

Synthesis of SLB736

The chemical and spectroscopic data are as follows: m.p. 130°C; ^{1}H NMR (400 MHz, CD_3OD) δ 8.35 (s, 1H), 4.53 (t, J = 7.2 Hz, 2H), 3.69 (s, 4H), 2.97 (td, J = 4.3, 8.0 Hz, 2H), 2.11 (td, J = 4.3, 8.0 Hz, 2H), 2.00–1.95 (m, 2H), 1.35–1.28 (m, 14H), 0.89 (t, J = 6.8 Hz, 3H); ^{13}C NMR (100 MHz, CD_3OD) δ 146.5, 127.3, 63.0 (2C), 62.6, 54.3, 33.8, 32.0, 31.5, 31.4, 31.3, 31.2, 30.8, 28.1, 24.5, 19.9, 15.2; IR (neat) υ_{max} = 3180, 2918, 2851, 2421, 1599, 1454, 1080, 1063, 958, 715 (cm^{-1}); HRMS (FAB) calcd. for $C_{17}H_{35}N_4O_2$ $[M-Cl^-]^+$ 327.2760, found 327.2762.

Treatment with SLB736 or FTY720 in vivo

Mice were administrated SLB736, FTY720 (1 mg/kg body weight each) or vehicle (0.9% NaCl) via oral gavage every day for 5 days/week for the indicated periods. After the indicated period of treatment, the mice were fasted for overnight and sacrificed. The liver tissues were quickly removed and kept frozen at -70°C for subsequent analysis.

SLB736 treatment *in vitro*

Hepatic macrophages were treated with chemicals at the indicated doses or sterile water (control) for

2 h. After washing twice with PBS, the cells were stimulated with LPS (L2880, Sigma-Aldrich) at a concentration of 100 ng/ml for 3 h, and then 1 mM ATP (A6419, Sigma-Aldrich) was added for 30 min.

Determination of S1PR4 localization in C6 glioma cell line

Stable C6 glioma cells expressing EGFP-conjugated S1PR4 were prepared by infection with retrovirus bearing S1PR4-EGFP fusion construct (kindly provided by Dr. Jerold Chun at The Sanford Burnham Prebys). S1PR4 internalization and recycling were assessed as previously described.[44] In brief, cells were plated on poly-$_L$-lysine (100 μg/mL)-coated coverslips, cultivated, serum-deprived, and then used for experiments. The cells were treated with vehicle (0.1% fatty acid-free BSA), S1P, FTY720-P, or SLB736 for 0.5 h; in some cases, the cells were washed and further incubated in the presence of cycloheximide (5 μg/mL) for 2 h or 4 h. At the end of each experiment, the cells were fixed in 4% paraformaldehyde and mounted with Vectashield. S1PR4 localization in cells was assessed by detecting the EGFP signal using a laser scanning confocal microscopy (Eclipse A1+, Nikon, Tokyo, Japan).

S1PR β-arrestin assay

β-arrestin recruitment assays for S1PR activity were performed by DiscoveRx (Fremont, CA).

Blood lymphocyte measurement

Blood lymphocytes were counted using an automated hematology analyzer (ADVIA 2120i 53, Siemens Healthcare Diagnostics, Tarrytown, NY).

Statistical analysis

Data are expressed as mean ± standard error of the mean (SEM). Unpaired two-tailed Student's *t*-tests were used to compare variables between groups, and one-way ANOVA was used to compare variables among multiple groups. Bonferroni correction was applied for post hoc analysis of the multiple comparisons. All statistical tests were conducted according to two-sided sample sizes and were determined on the basis of previous experiments that used similar methodologies. For all experiments, the stated replicates are biological replicates. Statistical analysis and graphing were performed using IBM SPSS Statistics for Windows version 22.0 (IBM Corp., Armonk, NY, USA) or GraphPad Prism 7 (GraphPad Software, La Jolla, CA, USA).

Results

S1PR4 expression is increased in the liver of diet-induced murine models of NASH

We first investigated which type of S1PR isoforms is activated in the murine models of NASH. HFHCD-feeding is one of the animal models that closely resemble the clinical characteristics of NASH[43,45,46]. We also used the methionine- and choline-deficient diet (MCDD), Western diet (WD) and choline deficient, L-amino acid-defined, high-fat diet (CDA+HFD)[47]. Interestingly, S1pr4 was the only isoform that consistently showed increased mRNA expression in the livers of mice fed HFHCD, MCDD, WD, or CDA+HFD; the expression of S1pr1 and S1pr2 were only increased in mice fed WD, and that of S1pr3 expression was only increased in mice fed HFHCD, MCDD or WD (Figure 1A). Next, we measured the S1PR4 expression in liver from patients with NASH. In parallel, NASH patients exhibited increased higher S1PR4 expression (Figure 1B).

S1PR4 is the key mediator of NASH development

We thus tested the possible involvement of S1PR4 in the development of NASH by using genetic modulation. HFHCD-fed heterozygous *S1pr4* KO mice (*S1pr4*$^{+/-}$ mice) showed significantly lower degrees of hepatic inflammation and fibrosis, compared with HFHCD-fed wild type (WT) mice (Figure 2*A, B*); However, the degree of hepatic steatosis was similar regardless of the *S1pr4* genotype (Figures 2*C*). Also, we observed a trend towards increase in the expression of both *S1pr4* expression and genes involved in inflammation (Tumor necrosis factor-*α* (*Tnf)-α* and monocyte chemoattractant protein-1 (*Mcp1*)) in mice fed HFHCD for 4 and 12 weeks than in control mice; On the other hand, these changes were significantly decreased in the liver from *S1pr4*$^{+/-}$ mice (Figure 2*D, E*). In addition, *S1pr4* knockdown ameliorated HFHCD-induced liver fibrosis, lowered expression of transforming growth factor-β1 (*Tgf-β1*), α-smooth muscle actin (α-SMA) and Collagen Type III alpha 1 Chain (Col3a1) (Figure 2*F*). Collectively, these data indicate that S1PR4 is a critical mediator of the development of NASH.

S1PR4 is necessary for activation of the NLRP3 inflammasome in hepatic macrophages

NLRP3 inflammasome is involved in the pathogenesis of various inflammatory and metabolic diseases including arthritis, diabetes, and atherosclerosis[10,13] . Recent evidence also suggested that NLRP3 inflammasome activation in hepatic macrophages (Kupffer cells and monocyte-derived macrophages) is an important contributor to NASH and liver fibrosis[48], and blockade by a small molecule that antagonizes NLRP3 inflammasome or IL-1β was shown to reduce liver inflammation and fibrosis in alcoholic steatohepatitis and NASH in mice[16,49]. Therefore, we evaluated the role of the NLRP3 inflammasome in the *S1pr4*$^{+/-}$ mice. Compared with HFHCD-fed WT mice, HFHCD-fed *S1pr4*$^{+/-}$ mice exhibited significantly decreased NLRP3 inflammasome markers in the liver (Figure 3*A*). S1PR4 was reported to be specifically expressed in myeloid cells such as dendritic cells and macrophages[50,51]; however, its role in the pathogenesis of NASH is largely unknown. To address which cell types are responsible for this S1PR4 upregulation, we examined the expression levels of *S1pr4* in primary hepatocytes, hepatic macrophages, and HSCs. *S1pr4* expression was rarely detected in hepatocytes and HSCs (Figure 3*B*); in contrast, *S1pr4* expression was significantly higher in

hepatic macrophages isolated from HFHCD-fed mice for 4 weeks than those isolated from control mice (Figure 3*B*).

To explore the relationship between high *S1pr4* expression and NLRP3 inflammasome in hepatic macrophages, we isolated hepatic macrophages from *S1pr4*$^{+/-}$ mice. Hepatic macrophages from *S1pr4*$^{+/-}$ mice had a significantly lower degree of lipopolysacchardie (LPS)- and ATP-induced increases in interleukin-1 (IL-1) β production (Figure 3*C*). These results suggest that S1PR4 is necessary for NLRP3 inflammasome activation in hepatic macrophages. The activation of NLRP3 inflammasome is achieved through two sequential steps—signal 1 (priming) and signal 2 (activation)[52]: signal 1 is provided by microbial molecules or endogenous cytokines and leads to the upregulation of NLRP3 and pro-IL-1β through the activation of the transcription factor NF-kB, and signal 2 is triggered by ATP, pore-forming toxins, viral RNA, and particulate matters. Interestingly, LPS-induced increases in *Nlrp3* and *Pro-IL-1β* were significantly nullified in *S1pr4*$^{+/-}$ hepatic macrophages (Figure 3*D*). Also, the phosphorylation of NF-kB in LPS-primed *S1pr4*$^{+/-}$ hepatic macrophages was decreased (Figure 3*E*), suggesting that S1PR4 activates the NLRP3 inflammasome from signal 1.

S1PR4-dependent calcium release from ER plays a pivotal role in the NLRP3 inflammasome activation in hepatic macrophages

Intracellular ions such as K^+, Ca^{++}, and Cl^- have significant roles in the activation of the NLRP3 inflammasome[53]. Among them, intracellular Ca^{++} signaling plays one of the major roles in the activation of NLRP3 inflammasomes[54]. Accordingly, treatment with the [Ca^{++}] chelator BAPTA-AM in hepatic macrophages significantly decreased the IL-1β production in response to LPS- and ATP-stimulation as well as the LPS-induced increases in the expression of *Nlrp3* and Pro-*IL-1β* (Figure 4*A-C*).

A previous study indicated that phospholipase C (PLC)-dependent changes in [Ca^{++}] is the downstream signaling of S1PR4[55]. Activation of PLC triggers the release of inositol trisphosphate (IP_3) from phosphatidylinositol 4, 5-bisphosphate, and [Ca^{++}] is released to the cytosol when IP_3 interacts with IP_3 receptor (IP_3R) located at the endoplasmic reticulum (ER) membrane[56]. In our experimental setting, treatment with PLC inhibitor U73122 or IP3R inhibitors Xes-c and 2-APB significantly decreased the LPS-mediated increases in the expression levels of *Nlrp*3 and *Pro-IL-1β* (Figure 4*A* and *D-E*) as well as the production of IL-1β in response to LPS- and ATP-stimulation (Figure 4*F*). Taken together, these results indicate that increases in [Ca^{++}] release from the ER through the PLC/IP_3R axis play an important role in the activation of the NLRP3 inflammasome in hepatic macrophages. LPS-induced increase in the level of IP_3 (IP-one), the product of PLC[57], was significantly decreased in *S1pr4*$^{+/-}$ cells (Figure 4*G*). Consistently, measurement of [Ca^{++}] showed that LPS treatment in hepatic macrophages induced a robust increase in [Ca^{++}] (Figure 4*H*), which is in line with previously reported data[58]. On the other hand, LPS-induced [Ca^{++}] release was significantly decreased in *S1pr4*$^{+/-}$ hepatic macrophages (Figure 4*H*). These results collectively indicate that S1PR4 is required for the calcium signaling associated with the NLRP3 inflammasome activation.

S1P activates the NLRP3 inflammasome by the S1PR4/PLC/IP_3 axis

We examined the possible role of the S1P/S1PR4 axis in the activation of the NLRP3 inflammasome.

S1P may emerge as the development of nonalcoholic fatty liver disease and liver fibrosis[59]. Sphingosine kinases (SK; SK1 and SK2) catalyze the formation of S1P from the precursor sphingosine.

Interestingly, expression of *Sk1* was markedly increased in the liver and in hepatic macrophages but not in hepatocytes of HFHCD-fed mice (Figure 5*A-C*). These data suggested that increased S1P levels may induce hepatic inflammation. To further explore the role of S1P on the activation of the NLRP3 inflammasome, hepatic macrophages were treated with S1P. S1P significantly increased the expression level of *S1pr4* in hepatic macrophages (Figure 5*D*). S1P also significantly increased the expression levels of *Nlrp3* and *Pro-IL-1β*, an effect that was dampened in *S1pr4*$^{+/-}$ hepatic macrophages (Figure 5*D*). S1P also stimulated the phosphorylation of NF-kB in hepatic macrophages, and this was reduced in *S1pr4*$^{+/-}$ hepatic macrophages (Figure 5*E*). Preteatment with BAPTA-AM, U73122, XesC, or 2-APB significantly reduced the S1P-mediated induction of *Nlrp3* and *Pro-IL-1β* expression (Figure 5*F*). These results suggest that extracellular S1P may act as a modulator of the NLRP3 inflammasome in hepatic macrophages through the PLC/IP_3/IP_3R signaling axis.

Development of a novel functional antagonist for S1PR4

In order to further clarify the biological function of S1PR4, we developed a chemical probe that selectively modulates S1PR4. We envisioned that introducing additional heteroatoms into the structure of FTY720 could change the selectivity for S1P subtype by referring to the X-ray crystal structure of S1PR1[60] and previous structural studies of S1PR4[61]. Accordingly, we designed and synthesized several types of heteroatom-containing analogues of FTY720. Among the designed analogues, a triazole-containing compound SLB736 (Figure 6*A*) showed a selective agonistic activity against S1PR4 (EDG6) based on β-arrestin recruitment assay (Figure 6*B*). The unique action of the currently used drugs targeting S1PRs, including FTY720 is the functional antagonism for S1PR1[62] in which S1PR1 is irreversibly internalized and degraded upon binding with FTY720-P, the phosphorylated active form of FTY720[44,62]. Downregulation of S1PR1 on T lymphocytes mediates the immunomodulatory effect of FTY720[63]. However, the possible functional antagonistic effects of FTY720-P or SLB736 on S1PR4 have not been investigated. We reasoned that the agonistic activity of SLB736 for S1PR4 as observed in β-arrestin recruitment assay may reflect functional antagonism. Therefore, we examined the localization of S1PR4 at different time points after the activation of S1PR4 in C6 glioma cells bearing EGFP-conjugated S1PR4. S1PR4 was internalized by brief exposure (0.5 h) to S1P, FTY720-P, or SLB736. Whereas S1PR4 was quickly recycled to the cell surface after the removal of S1P, S1PR4 remained in the cytoplasm until 2 h and 4 h after the removal of FTY720-P or SLB736 (Figure 6*C*). These data indicate that SLB736 and FTY720-P act as functional antagonists for S1PR4. Consistently, even at fairly low concentrations, SLB736 decreased the protein levels of S1PR4 in LPS-primed hepatic macrophages in a dose-dependent manner (Figure 6*D*).

SLB736 prevents the development of NASH and fibrosis

Similar to the previous study that used FTY720[40], administration of SLB736 to HFHCD-fed mice prevented the development of NASH and hepatic fibrosis (Figure 7*A* and *B*). Interestingly, the administration of SLB736 did not reduce the number of lymphocytes, which is a well-known adverse effect of FTY720 through its effect on S1PR1[41] (Figure 7*C*) . Whereas treatment with SLB736 did not

significantly reduce the diet-induced increases in the mRNA level of *S1pr4* (Figure 7*D*), the protein level of S1PR4 was significantly decreased upon treatment with SLB736 (Figure 7*E*), thus signifying that SLB736 carry functional antagonistic roles on S1PR4 *in vivo*. Whether SLB736 promotes S1PR4 protein instability or degradation remains to be established.

We further investigated whether SLB736 shows a similar preventive effect in other diet-induced murine models of NASH. We found that similar to HFHCD-fed mice, mice fed MCDD or CDA+HFD developed NASH along with increases in the expression of inflammation and inflammasome markers, which were effectively nullified by the administration of SLB736 (Figure 8*A-D*). To further demonstrate the therapeutic effect of SLB736, we administered SLB736 to mice fed MCDD for 4 weeks, a time point at which hepatic steatosis was evident (Figure 8*E*). Administration of SLB736 for 4 weeks ameliorated NASH and fibrosis in these mice (Figure 8*F*).

SLB736 suppresses the NLRP3 inflammasome in hepatic macrophages

We next checked the effect of SLB736 on the NLRP3 inflammasome in the hepatic macrophages. As expected, SLB736 decreased the production of IL-1β in response to LPS and ATP, and the expression of *Nlrp3* and *Pro-IL-1β* in response to LPS (Figure 9*A* and *B*). Consistently, LPS-induced increase in the level of IP_3 (IP-one), the product of PLC was significantly decreased in cells treated with SLB736 (Figure 9*C*). Pretreatment with SLB736 inhibited the LPS-induced [Ca^{++}] release in hepatic macrophages (Figure 9*D*). These data suggested that SLB736 as a functional antagonist of S1PR4 inactivates NLRP3 inflammasome and prevents NASH development.

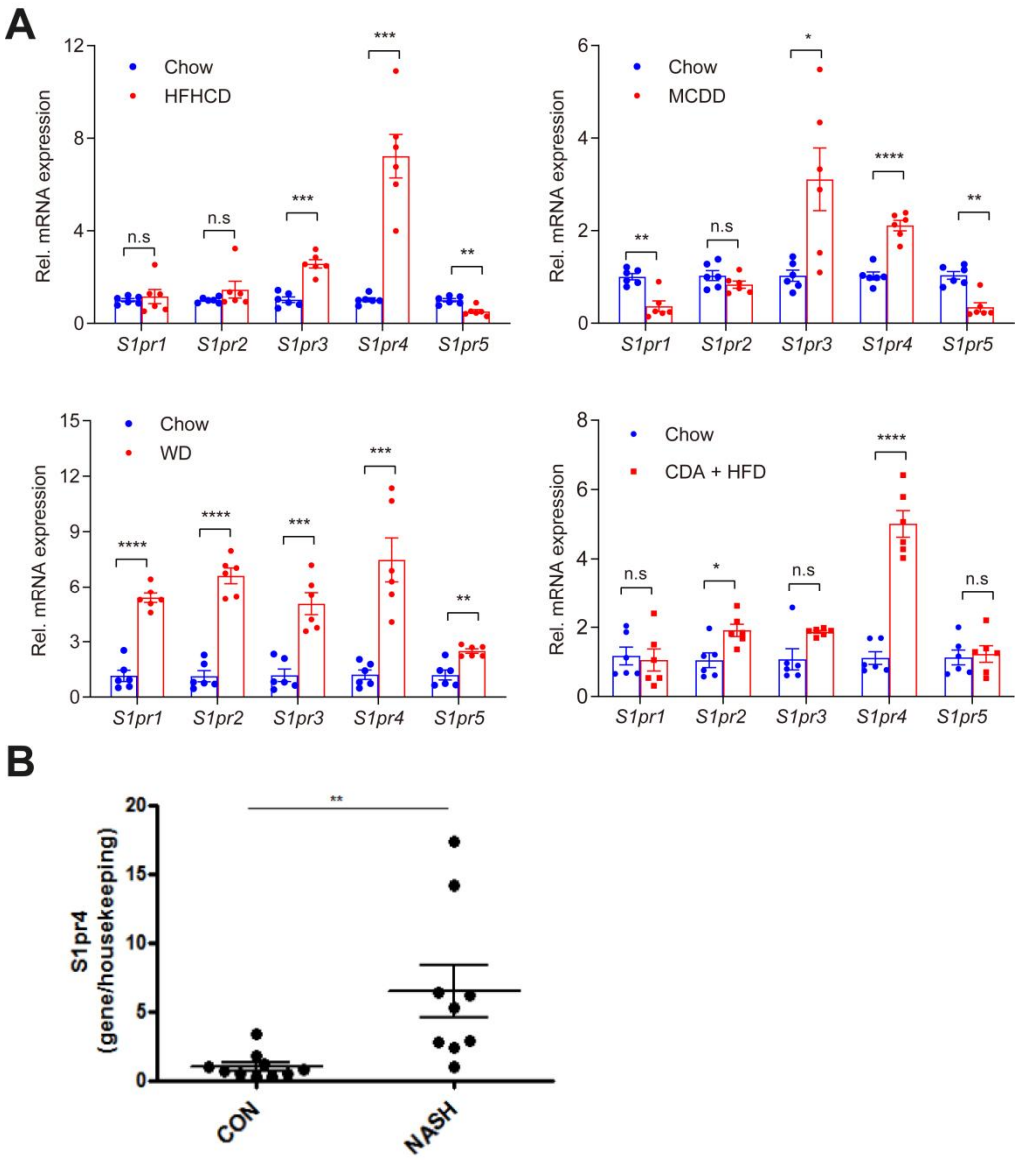

Figure 1. Hepatic S1pr4 expression is uniquely increased in the liver of murine NASH models and in NASH patients. Diet was administered to mice for 12 weeks for HFHCD, 8 weeks for MCDD, 16 weeks for WD, and 6 weeks for CDA + HFD. (*A*) Hepatic *S1pr* mRNA expression in HFHCD -, MCDD -, WD- and CDA+HFD-induced dietary models of NASH (n = 6). (B) Hepatic *S1pr* mRNA expression in liver samples of patients with NASH (n=9). Surgical specimens of donor livers were used as control (n=10) All data are shown as mean ± SEM. Data were analyzed Student's two-tailed unpaired *t*-test. ns, not significant, *$p < 0.05$, **$p < 0.01$, ***$p < 0.001$, ****$p < 0.0001$.

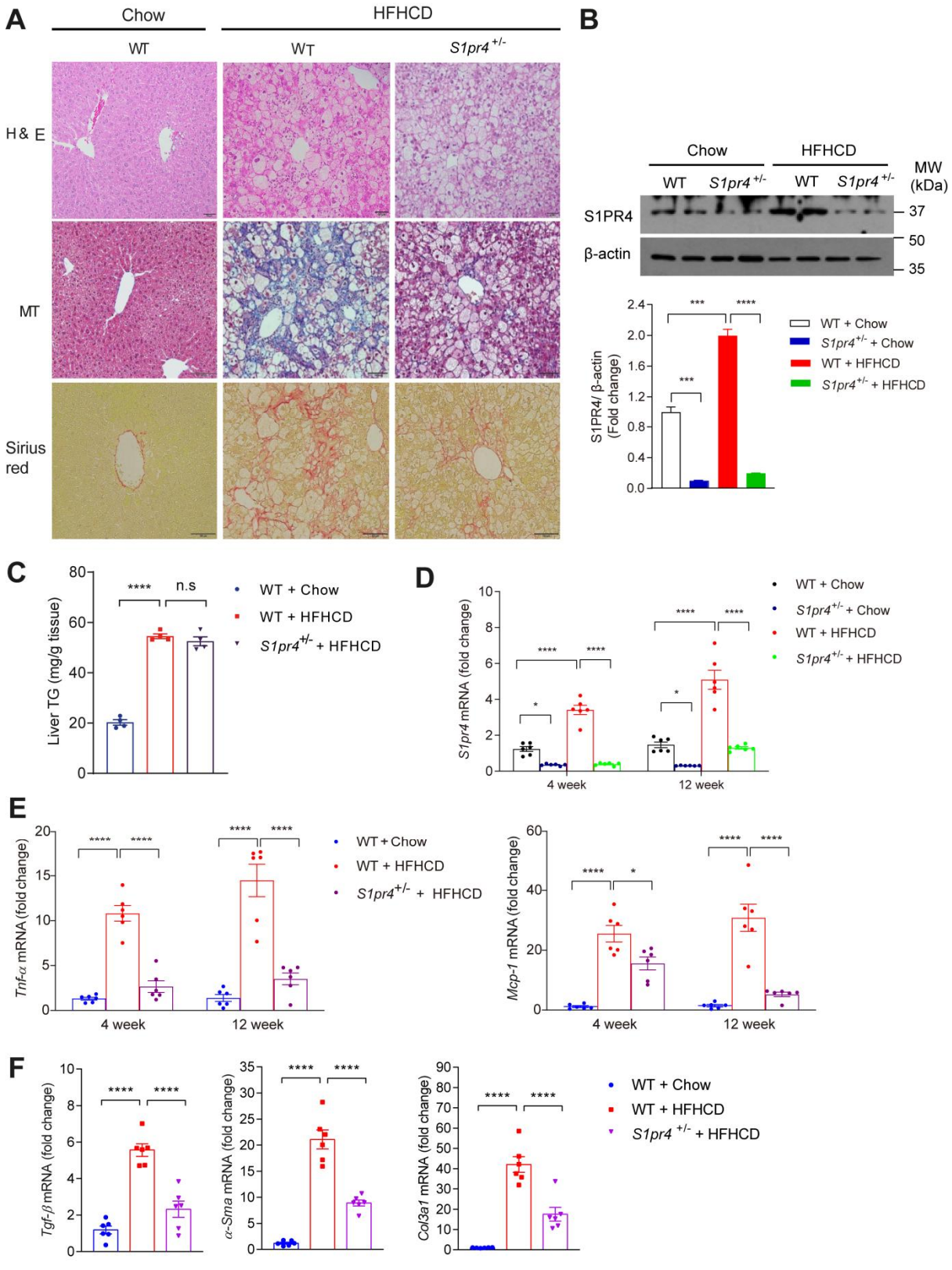
A
Chow
HFHCD
WT
WT
S1pr4 +/-
H& E
MT
Sirius red
B
Chow
HFHCD
WT
S1pr4 +/-
WT
S1pr4 +/-
MW (kDa)
S1PR4
β-actin
37
50
35
S1PR4/ β-actin (Fold change)
WT + Chow
S1pr4+/- + Chow
WT + HFHCD
S1pr4+/- + HFHCD
C
Liver TG (mg/g tissue)
****
n.s
WT + Chow
WT + HFHCD
S1pr4+/- + HFHCD
D
S1pr4 mRNA (fold change)
4 week
12 week
WT + Chow
S1pr4+/- + Chow
WT + HFHCD
S1pr4+/- + HFHCD
E
Tnf-α mRNA (fold change)
4 week
12 week
WT + Chow
WT + HFHCD
S1pr4+/- + HFHCD
Mcp-1 mRNA (fold change)
4 week
12 week
F
Tgf-β mRNA (fold change)
α-Sma mRNA (fold change)
Col3a1 mRNA (fold change)
WT + Chow
WT + HFHCD
S1pr4 +/- + HFHCD

Figure 2. S1PR4 is critical mediator of hepatic inflammation and fibrosis. *S1pr4*$^{+/-}$ mice were fed chow diet or HFHCD for 12 weeks. (*A*) Representative H&E, MT and Sirius-red staining in liver tissues. Scale bar, 50 μm. Hepatic S1PR4 mRNA (*B*) and protein (*C*) expression in the *S1pr4*$^{+/-}$ mice fed with HFHCD (n = 6). The S1PR4 protein was normalized to β-actin. (*D, E*) Relative mRNA expression levels of the genes associated with inflammation (*Tnf-α, Mcp-1*) and fibrosis (*Tgf-β, α-Sma, Col3al*) (n = 6). All data are shown as mean ± SEM. Data in *B-E* were analyzed by one-way ANOVA with Bonferroni correction. *$p < 0.05$, ***$p < 0.0005$, ****$p < 0.0001$.

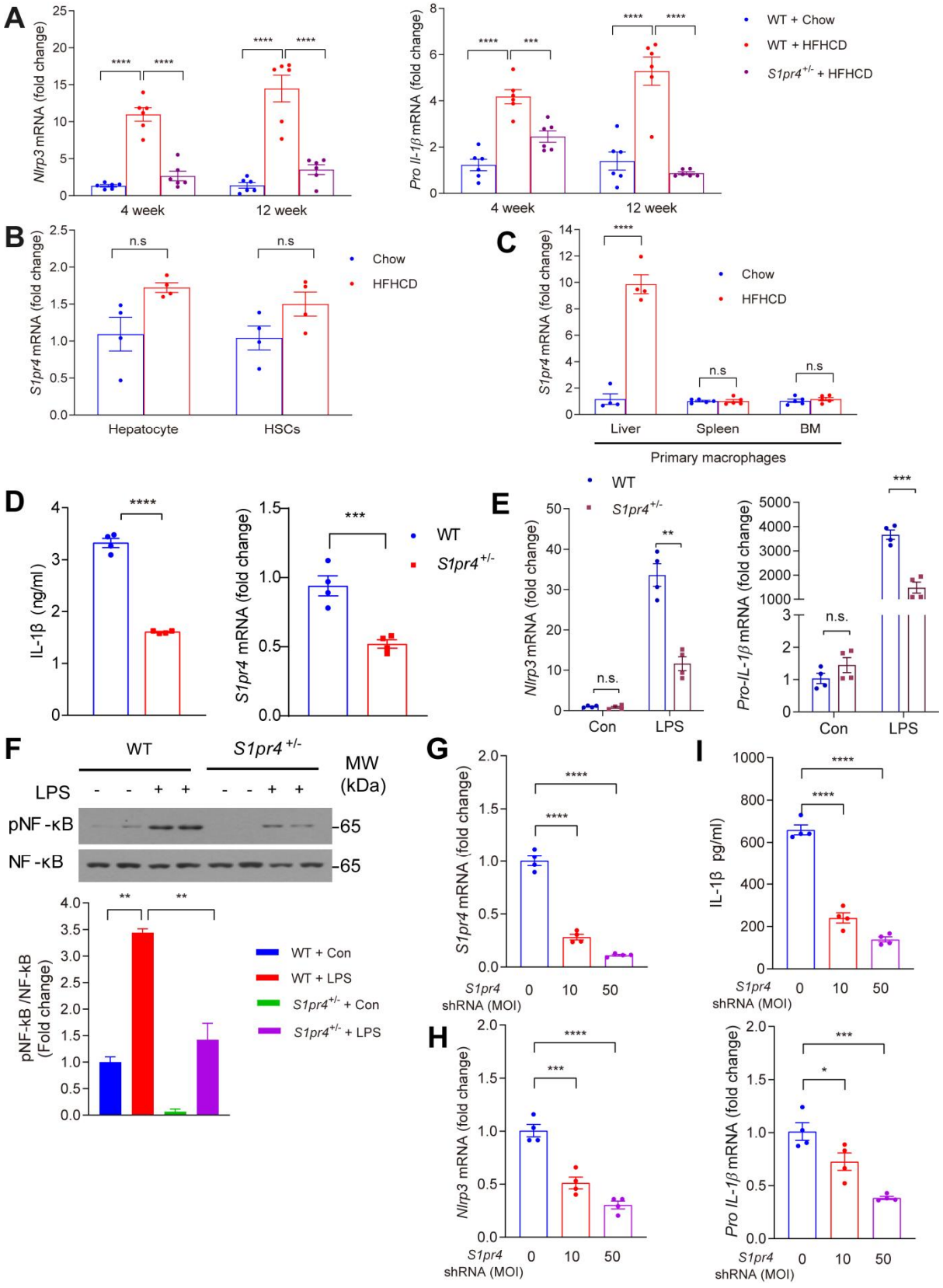
A
Nlrp3 mRNA (fold change)
4 week
12 week
Pro Il-1β mRNA (fold change)
WT + Chow
WT + HFHCD
S1pr4+/- + HFHCD
B
S1pr4 mRNA (fold change)
n.s
Chow
HFHCD
Hepatocyte
HSCs
C
S1pr4 mRNA (fold change)
Liver
Spleen
BM
Primary macrophages
D
IL-1β (ng/ml)
S1pr4 mRNA (fold change)
WT
S1pr4+/-
E
Nlrp3 mRNA (fold change)
Pro-IL-1β mRNA (fold change)
Con
LPS
F
WT
S1pr4+/-
MW (kDa)
LPS
pNF-κB
NF-κB
-65
pNF-κB /NF-kB (Fold change)
WT + Con
WT + LPS
S1pr4+/- + Con
S1pr4+/- + LPS
G
S1pr4 mRNA (fold change)
S1pr4 shRNA (MOI)
H
Nlrp3 mRNA (fold change)
Pro IL-1β mRNA (fold change)
I
IL-1β pg/ml)

Figure 3. S1PR4 depletion decreases NLRP3 inflammasome activation in hepatic macrophages. (*A*) Relative hepatic mRNA expression levels of the genes associated with the components of NLRP3 inflammasome ($n = 6$). *S1pr4*$^{+/-}$ mice were fed chow or HFHCD for 12 weeks. (*B*) mRNA expression of *S1pr4* in primary hepatocytes, hepatic macrophages and HSCs from mice fed chow diet or HFHCD for 4 weeks ($n = 4$). (*C-E*) *S1pr4* depletion decreases NLRP3 inflammasome activation in he patic macrophages. (*C*) Hepatic macrophages isolated from *S1pr4*$^{+/-}$ mice were stimulated with LPS (100 ng/ml) for 3 h followed by ATP (1 mM) for 30 min. Cell culture media were collected and IL-1β levels were measured by ELISA ($n = 4$). (*D*) Relative mRNA expression levels of *Nlrp3* and *Pro-IL-1β* ($n = 4$) (*D*) and representative Western Blots of NF-kB phosphorylation and corresponding quantification ($n = 3$) (*E*). *S1pr4*$^{+/-}$ hepatic macrophages were stimulated with LPS (100 ng/ml) for 3 h (*D*) or 30 min (*E*). All data are shown as mean ± SEM. Data in *A* and *E* were analyzed by one-way ANOVA with Bonferroni correction. Data in *B-D* were analyzed by Student's two-tailed unpaired *t*-test. ns, not significant, $^{**}p < 0.01$, $^{***}p < 0.001$, $^{****}p < 0.0001$.

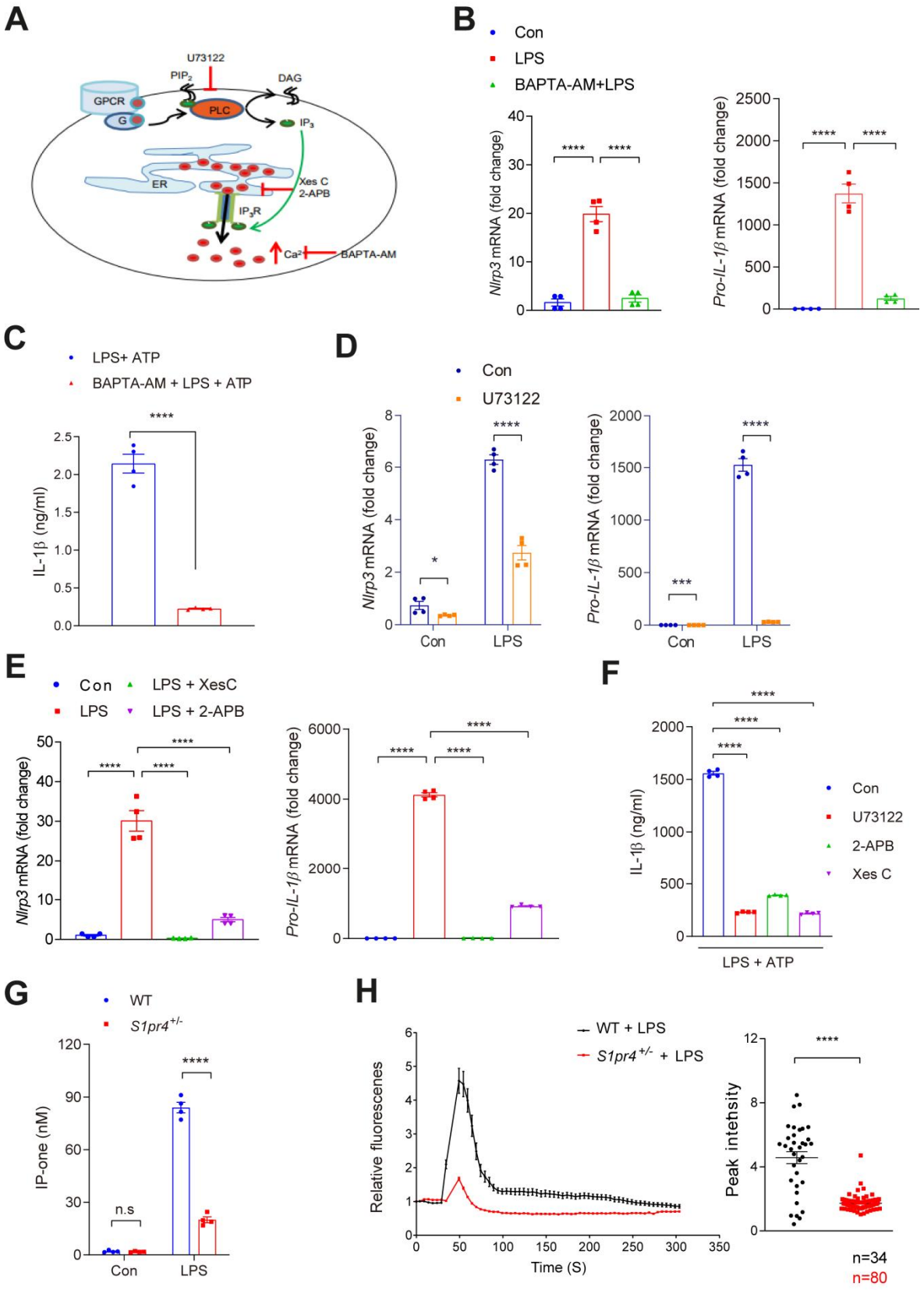
A
U73122
PIP2
DAG
GPCR
G
PLC
IP3
ER
Xes C
2-APB
IP3R
Ca2+
BAPTA-AM
B
Con
LPS
BAPTA-AM+LPS
Nlrp3 mRNA (fold change)
Pro-IL-1β mRNA (fold change)
C
LPS+ ATP
BAPTA-AM + LPS + ATP
IL-1β (ng/ml)
D
Con
U73122
Nlrp3 mRNA (fold change)
Pro-IL-1β mRNA (fold change)
Con
LPS
E
Con
LPS
LPS + XesC
LPS + 2-APB
Nlrp3 mRNA (fold change)
Pro-IL-1β mRNA (fold change)
F
IL-1β (ng/ml)
Con
U73122
2-APB
Xes C
LPS + ATP
G
WT
S1pr4+/-
IP-one (nM)
n.s
Con
LPS
H
WT + LPS
S1pr4+/- + LPS
Relative fluorescenes
Time (S)
Peak intesity
n=34
n=80

Figure 4. Intracellular calcium signaling is necessary for S1PR4-dependent activation of NLRP3 inflammasome in hepatic macrophages. (*A*) Schematic illustration of inhibitor of PLC and IP_3. (*B*, *C*) Effect of calcium depletion on LPS-induced activation of NLRP3 inflammasome. Relative mRNA expression levels of *Nlrp3* and *pro-IL-1β* in the cells (*B*) and IL-1β secretion into the culture medium (n = 4) (*C*). Hepatic macrophages were pre-treated with BAPTA-AM (10 μM) for 30 min and then treated with LPS (100 ng/mL) for 3 h (*B*). In another set of experiments, LPS-primed hepatic macrop hages were treated with ATP (1 mM) for 30 min (*C*). (*D-F*) Inhibition of LPS-induced NLRP3 inflammasome pathway by suppression of the PLC/IP_3/IP_3R axis. (*D*) Relative mRNA expression levels of *Nlrp3* and *pro-IL-1β*. Hepatic macrophages were treated with 10 μM U73122 (*D*), 5 μM Xes C or 100 μM 2-APB (n = 4) (*E*). (*F*) IL-1β in the culture medium. Hepatic macrophages pre-treated with U73122 (10 μM), Xes C (5 μM), or 2-APB (100 μM) for 30 min and DMSO as vehicle control. Hepatic macrophages were treated with 1 mM ATP for 30 min after 3 h of LPS priming (100 ng/mL). IL-1β secreted in the culture supernatants was quantified by ELISA (n = 4). (*G, H*) S1PR4-dependent calcium release from ER plays a pivotal role in the priming of NLRP3 inflammasome in he patic macrophages. (*G*) Levels of IP-one in *S1pr4*$^{+/-}$ hepatic macrophages (n = 4). (*H*) Effect of S1PR4 on LPS-mediated [Ca^{++}] release. WT or *S1pr4*$^{+/-}$ hepatic macrophages were incubated with Fluo-4/AM followed by stimulation with LPS for 2 h. [Ca^{++}] was analyzed by time-lapse confocal microscopy (left panel). Quantification of LPS-induced peak fluorescent intensities (right panel). All data are shown as mean ± SEM. Data in *C*, *D*, *G* and *H* were analyzed by Student's two-tailed unpaired *t*-test. Data in *B*, *E* and *F* were analyzed by one-way ANOVA with Bonferroni correction. ns, not significant, *$p < 0.05$, ***$p < 0.001$, ****$p < 0.0001$.

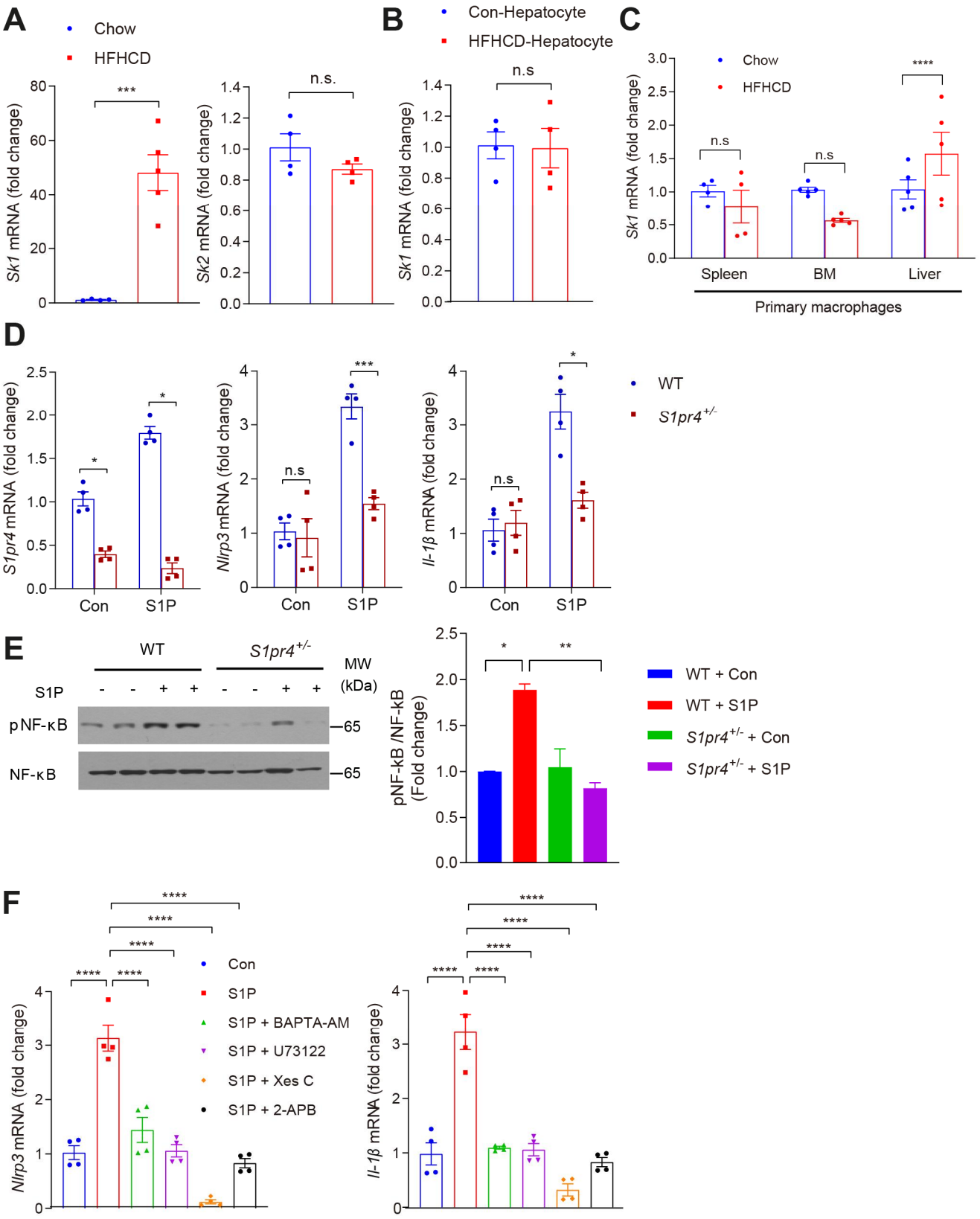
A
Chow
HFHCD
Sk1 mRNA (fold change)
Sk2 mRNA (fold change)
n.s.
B
Con-Hepatocyte
HFHCD-Hepatocyte
Sk1 mRNA (fold change)
n.s
C
Chow
HFHCD
Sk1 mRNA (fold change)
Spleen
BM
Liver
Primary macrophages
D
S1pr4 mRNA (fold change)
Nlrp3 mRNA (fold change)
Il-1β mRNA (fold change)
Con
S1P
WT
S1pr4+/-
E
WT
S1pr4+/-
MW (kDa)
S1P
pNF-κB
NF-κB
65
pNF-kB /NF-kB (Fold change)
WT + Con
WT + S1P
S1pr4+/- + Con
S1pr4+/- + S1P
F
Nlrp3 mRNA (fold change)
Il-1β mRNA (fold change)
Con
S1P
S1P + BAPTA-AM
S1P + U73122
S1P + Xes C
S1P + 2-APB

Figure 5. S1P activates NLRP3 inflammasome through S1PR4. (*A*) *Sk1* and *Sk2* mRNA expression in the livers of mice fed HFHCD for 12 weeks ($n = 4$). (*B, C*) *Sk1* mRNA expression in hepatic macrophages (*B*) and primary hepatocytes (*C*) from mice fed HFHCD for 4 weeks ($n = 4$). (*D, E*) *S1pr4* knockdown decreases the S1P-induced NLRP3 inflammasome activation. (*D*) The mRNA expression of *S1pr4*, *Nlrp3*, and *Pro-IL-1β*. Serum-starved $S1pr4^{+/-}$ hepatic macrophages were treated with S1P (1 μM) for 2 h ($n = 4$). (*E*) Representative Western Blots of NF-kB phosphorylation and corresponding quantification ($n = 3$). $S1pr4^{+/-}$ hepatic macrophages were treated with S1P (1 μM) for 30 min. (*F*) mRNA expression of *Nlrp3* and *Pro-IL-1β*. Serum-starved hepatic macrophages were treated with BAPTA-AM (10 μM), U73122 (10 μM), Xes C (5 μM), or 2-APB (100 μM), and treated with S1P (1 μM) ($n = 4$). All data are shown as mean ± SEM. Data in *A-D* were analyzed by Student's two-tailed unpaired *t*-test. Data in *E* and *F* were analyzed by one-way ANOVA followed by Bonferroni correction. ns, not significant, $*p < 0.05$, $**p < 0.01$, $***p < 0.001$, $****p < 0.0001$.

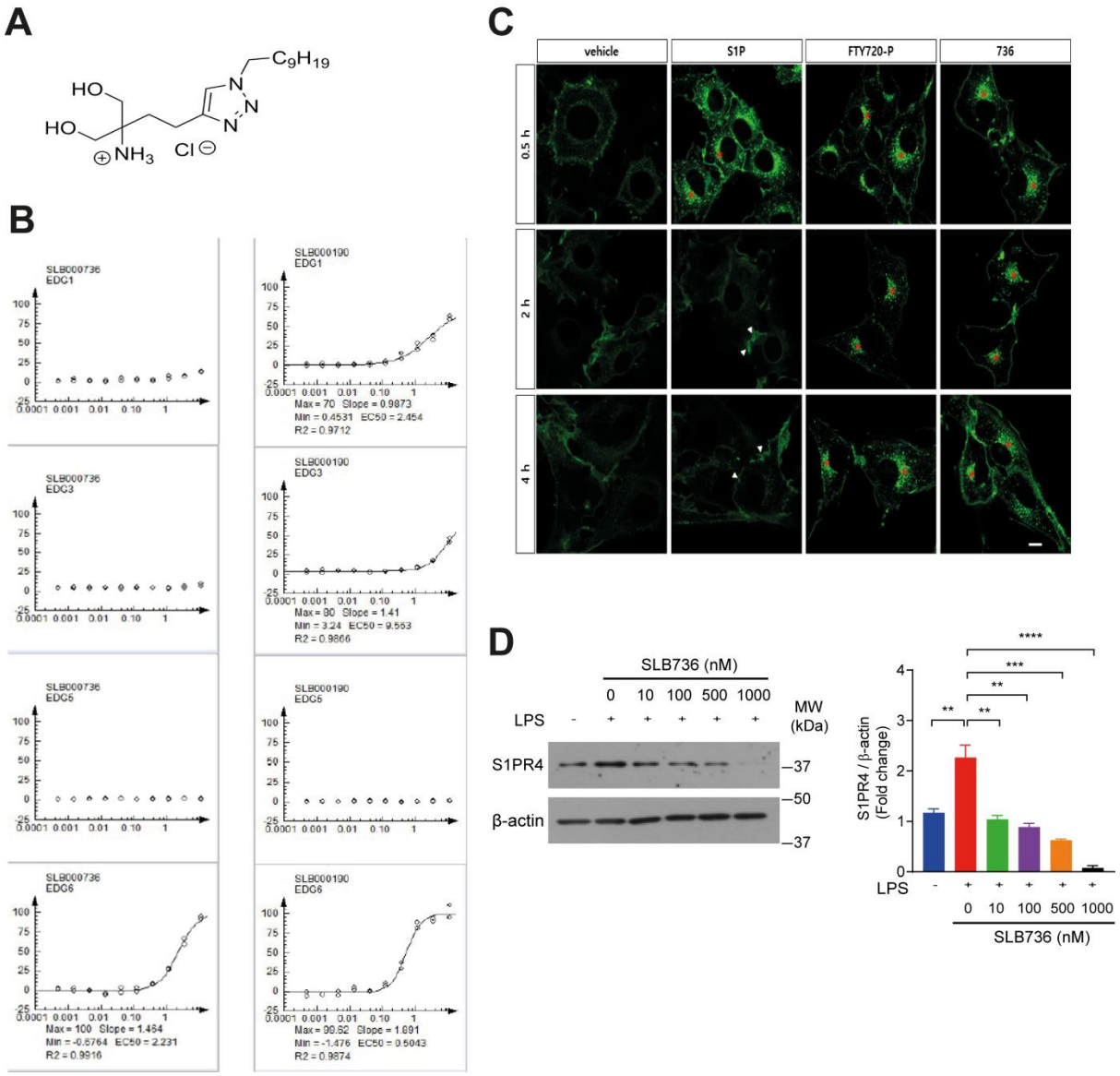

Figure 6. SLB736 acts as a functional antagonist of S1PR4. (*A*) Structure of SLB736. (*B*) Isoform-specific S1PR activity of SLB736. β-arrestin PathHunter® assay was performed in the clonal S1PR/HEK293 cell line in the presence of SLB736 (left) and FTY720-P (right). EDG 1 = S1PR1, EDG5 = S1PR2, EDG3 = S1PR3, EDG6 = S1PR4. (*C*) S1PR4 internalization and recycling were assessed in C6 glioma cells overexpressing EGFP-fused S1PR4. Cells were exposed to vehicle (0.1% BSA), S1P (100 nM), FTY720-P (1 μM), or SLB736 (1 μM) for 0.5 h and fixed. Cells exposed to reagents for 0.5 h were washed and further incubated with vehicle in the presence of cyclohexamide for up to 4 h. Asterisks or arrowheads indicate cytosolic locations or the cell surface. Scale bar, 10 μm. (*D*) Protein level of S1PR4 in hepatic macrophages. The S1PR4 protein was normalized to β-actin. Hepatic macrophages were pre-treated with SLB736 at the indicated dose and then treated with 100 ng/ml of LPS for 24 h ($n = 4$). All data are shown as mean ± SEM. Data in D were analyzed by one-way ANOVA followed by Bonferroni correction. $^{**}p < 0.01$, $^{***}p < 0.001$, $^{****}p < 0.0001$.

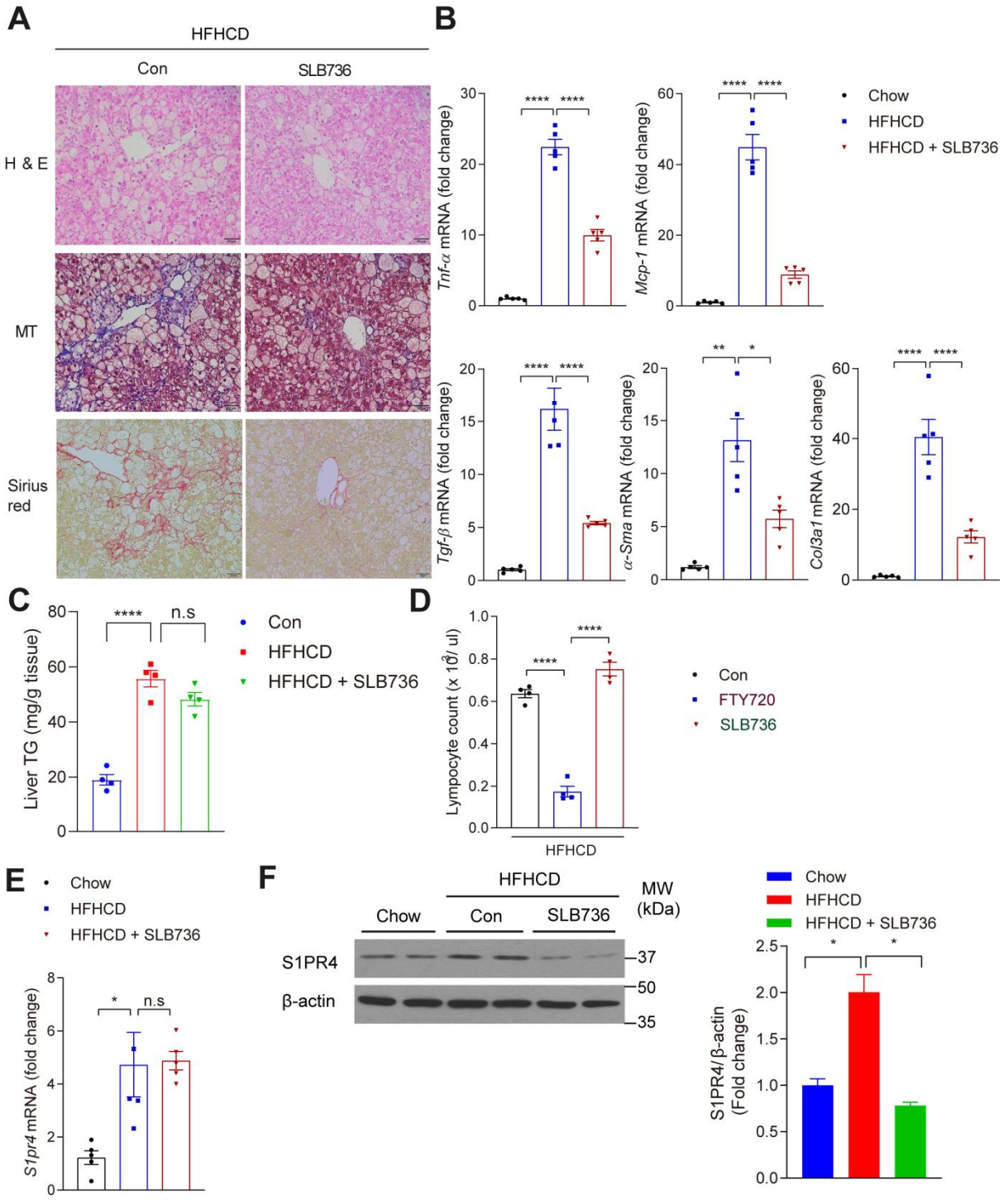

Figure 7. SLB736 treatment prevents HFHCD-induced NASH. (*A*) Representative H&E, MT, and Sirius Red staining of the livers. Scale bars, 50 μm. SLB736 (1 mg/kg/day) was administered for 12 weeks in HFHCD-fed mice. (*B*) Relative mRNA expression levels of the genes associated with inflammation (*Tnf-α, Mcp-1*) and fibrosis (*Tgf-β, α-Sma, Col3al*) in the livers of HFHCD-fed mice with or without SLB736 treatment (n = 5). (*C*) Lymphocyte counts in the blood. FTY720 or SLB736 (1 mg/kg/day) were administered for 12 weeks in HFHCD-fed mice (n = 4). (*D, E*) mRNA expression of *S1pr4* (*D*) and representative Western blots of S1PR4 and corresponding quantification (*E*) in the

liver of HFHCD-fed mice treated with SLB736 (n = 4). All data are shown as mean ± SEM. Data in *B-E* were analyzed by one-way ANOVA followed by Bonferroni correction. ns, not significant, *p < 0.05, **p < 0.01, ****p < 0.0001.

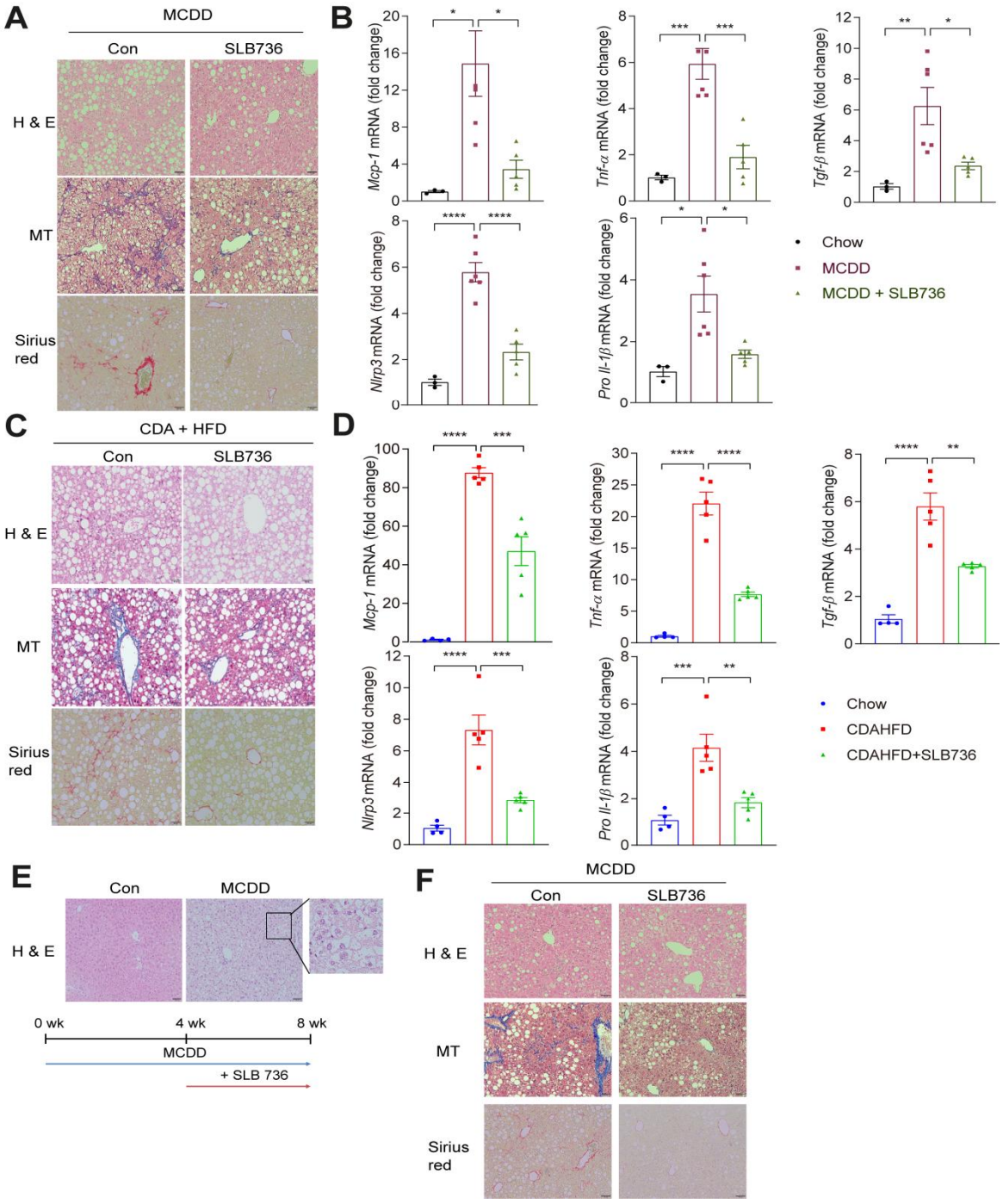

Figure 8. SLB736 prevents NASH in other animal models and retards the progression to NASH and fibrosis. (*A*) Representative H&E, MT, and Sirius Red staining of the livers of MCDD-fed mice with or without SLB736 treatment for 8 weeks. Scale bars, 50 μm. (*B*) Relative mRNA expression levels of inflammation, fibrosis and inflammasome markers in the livers of chow-fed mice and MCDD-fed mice with or without SLB736 (n = 5–6). (*C*) Representative H&E, MT, and Sirius Red staining of the livers of CDA+HFD-fed mice with or without SLB736 treatment for 6 weeks. Scale bars, 50 μm. (*D*) Relative mRNA expression levels of markers for inflammation, fibrosis and inflammasome in the livers of chow-fed mice and CDA+HFD-fed mice with or without SLB736 treatment (n = 4–5). (*E*) Representative H & E of livers of MCDD-fed mice for 4 weeks. Scale bars,

50 μm. Inlet shows the lipid accumulation in hepatocytes. The lower panel describes the schematic schedule for observing the therapeutic effect of SLB736 in MCDD-fed mice. (*F*) Representative H&E, MT, and Sirius Red staining of the livers. Scale bars, 50 μm. After feeding MCDD for 4 weeks, SLB736 (1 mg/kg/day) was administrated for 4 weeks with MCDD. All data are shown as mean ± SEM. Data in B and D were analyzed by one-way ANOVA followed by Bonferroni correction. *$p < 0.05$, **$p < 0.01$, ***$p < 0.001$, ****$p < 0.0001$.

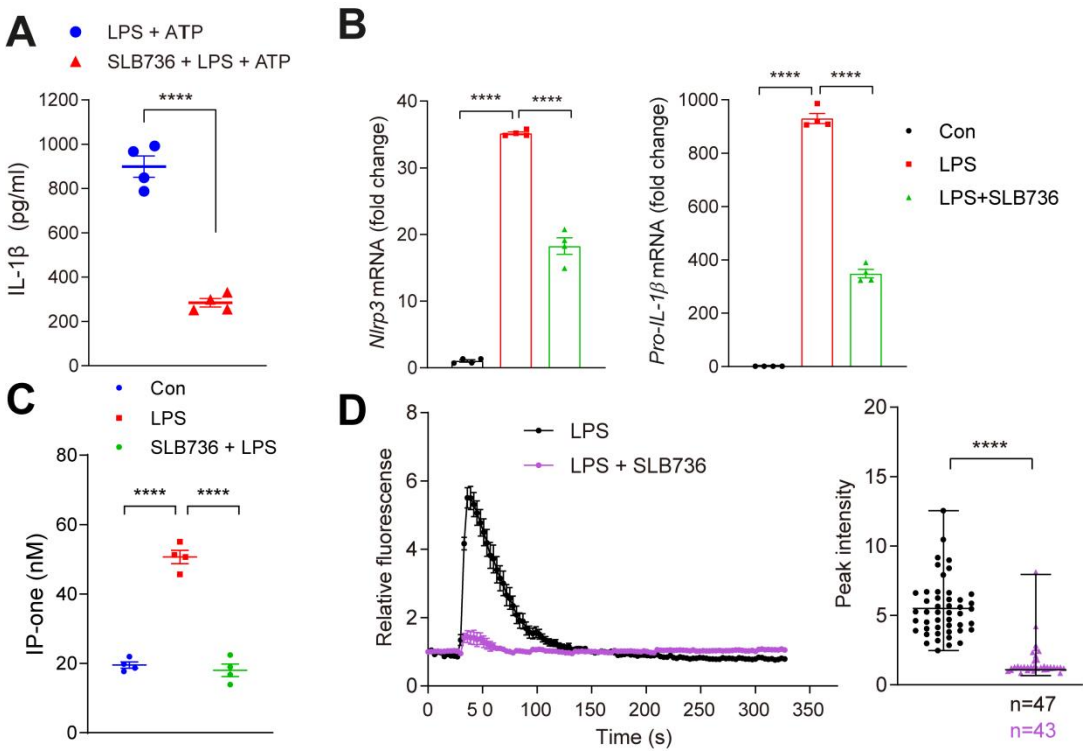

Figure 9. **SLB736 decreases NLRP3 inflammasome activation in hepatic macrophages.** (*A*) IL-1β levels in the culture media of hepatic macrophages. Hepatic macrophages were pre-treated with 1 μM SLB736 for 2 h, and treated with LPS 100 ng/ ml for 3 h followed by ATP (1 mM) for 30 min. (*B*) Relative mRNA expression of *Nlrp3* and *Pro-IL-1β*. Hepatic macrophages were pre-treated with 1 μM SLB736 for 2 h, and treated with LPS 100 ng/ ml for 3 h (n = 4). (*C*) IP-one levels in hepatic macrophages. Cells were pre-treated with 1 μM SLB736 or vehicle for 2 h. (n = 4). The levels of IP-one in cell lysates was measured using by ELISA kit. (*D*) Effect of SLB736 on LPS-mediated [Ca^{++}] release. Hepatic macrophages were pre-treated with 1 μM SLB736 or vehicle for 2 h. Cells were then incubated with Fluo-4/AM followed by stimulation with LPS. [Ca^{++}] was analyzed by time-lapse confocal microscopy (left panel). Quantification of LPS-induced peak fluorescent intensities (right panel). All data are shown as mean ± SEM. Data *A* and *D* were analyzed by Student's two-tailed unpaired *t*-test. Data in *B* and *C* were analyzed by one-way ANOVA with Bonferroni correction. ****$p < 0.0001$.

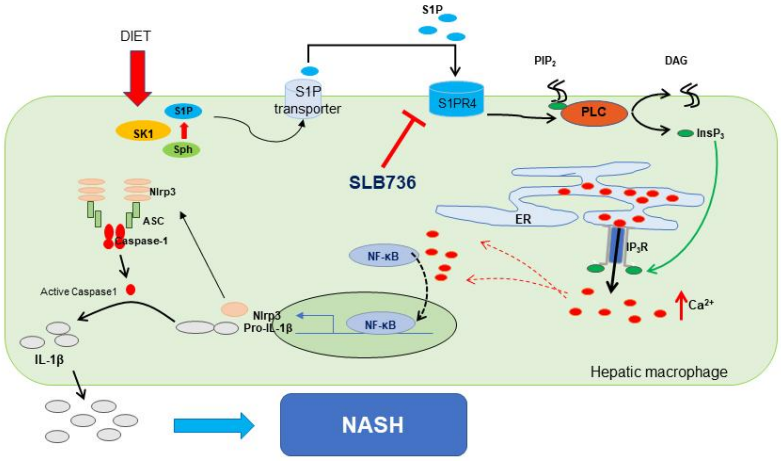

Figure 10. Conceptual model depicting the role of the SK1/S1PR4 axis in the pathogenesis of NASH. S1P produced by SK1 from hepatic macrophages induces S1PR4 in a paracrine manner, which is necessary for the [Ca^{++}]-dependent priming of the NLRP3 inflammasome.

Discussion

S1PR4 is specifically expressed in myeloid cells such as dendritic cells and macrophages[50,51]. S1PR4 is also required for the differentiation of plasmacytoid dendritic cells[50] and regulates the production of interferon-α thereof[64]. However, compared with other S1PRs, our knowledge of the physiological relevance of S1PR4 has been modest[63]. We found that the *S1pr4* expression was significantly higher in the livers of diet-induced NASH models and genetic depletion of *S1pr4* protected the mice agai nst hepatic inflammation and fibrosis. Hepatocyte death and inflammation is the critical trigger of NASH, which sequentially activates HSCs[65,66]. Interestingly, *S1pr4* expression was significantly induced by HFHCD feeding in hepatic macrophages, whereas it was rarely detected in hepatocyte and HSCs. A recent study reported that S1PR2 is involved in the NLRP3 inflammasome activation in hepatic macrophages during chronic liver injury[31]. In the present study, we found that S1PR4 in hepati c macrophages also plays an important role in the pathogenesis of NASH by activating the NLRP3 inflammasome. Expression of *S1pr4* was significantly increased in the liver of various mouse models of NASH. This is in line with a previous study that reported the upregulation of S1PR4 in human samples of liver cirrhosis[20].

As a major reservoir of intracellular [Ca^{++}], the ER plays a critical role in the regulation of intracellular [Ca^{++}] regulation[56]. Activation of the IP_3R, a Ca^{++}-release channel on the ER surface, is triggered by IP_3, a product of PLC-mediated phosphatidylinositol 4, 5-bisphosphate cleavage. We found that LPS sequentially activated PLC and IP_3R in hepatic macrophages to increase [Ca^{++}] and to activate the NLRP3 inflammasome, and that this reaction was abrogated by genetic depletion of *S1pr4* or treatment with SLB736. In addition to LPS, we found that S1P can also activate the NLRP3 inflammasome. Interestingly, expression of *Sk1* was selectively induced in hepatic macrophages by HFHCD feeding, and S1P increased the expression of *S1pr4* in hepatic macrophages. Accordingly, a previous study showed that the overloading of saturated fatty acids induces *Sk1* in hepatocytes to initiate proinflammatory signaling[67]. On the other hand, in HFHCD-fed mice, *Sk1* expression was induced in hepatic macrophages but not in hepatocytes. We thus suggest that S1P produced by SK1 from hepatic macrophages induces S1PR4 in a paracrine manner to activate the NLRP3 inflammasome (Figure 10).

We designed and synthesized heteroatom-containing FTY720 analogues with the aims of obtaining high S1PR4 activity and subtype selectivity. Among the synthesized analogues, SLB736 exhibited an excellent subtype selectivity and functional antagonism for S1PR4. The administration of SLB736 prevented the development of NASH and fibrosis. The protein levels of S1PR4 in the liver were significantly decreased by SLB736. Notably, SLB736 did not induce lymphopenia, a potentially serious side effect of FTY720 arising from its action on S1PR1[41,68].

NAFLD occurs mostly in obese individuals, and insulin resistance and deregulation of the lipid metabolism increase the risk of NAFLD and NASH[1]. Although lifestyle modification is the first-line treatment for patients with NASH, it is usually unsuccessful. Therefore, many agents for the treatment of NASH by targeting different pathways are under development[69], and several compounds have shown promising histologic results in phase IIa studies[3,70]. However, it was pointed out that histologic NASH is not an independent predictor of long-term mortality and that the stage of fibrosis is the only robust and independent predictor of liver-related mortality[3,71]. In this regard, targeting the NLRP3

inflammasome activation, which plays a central role in hepatic inflammation and fibrosis is increasingly recognized as a promising strategy for developing an efficient therapy against NASH[16,49]. In accordance, our study showed that SLB736 was effective in preventing the development of NASH and fibrosis by deactivating the NLRP3 inflammasome.

References

1. Friedman, S.L., Neuschwander-Tetri, B.A., Rinella, M. & Sanyal, A.J. Mechanisms of NAFLD development and therapeutic strategies. *Nature medicine* **24**, 908-922 (2018).
2. Lassailly, G., Caiazzo, R., Pattou, F. & Mathurin, P. Perspectives on Treatment for Nonalcoholic Steatohepatitis. *Gastroenterology* **150**, 1835-1848 (2016).
3. Younossi, Z.M., *et al.* Current and future therapeutic regimens for nonalcoholic fatty liver disease and nonalcoholic steatohepatitis. *Hepatology* **68**, 361-371 (2018).
4. Brunt, E.M., *et al.* Portal chronic inflammation in nonalcoholic fatty liver disease (NAFLD): a histologic marker of advanced NAFLD-Clinicopathologic correlations from the nonalcoholic steatohepatitis clinical research network. *Hepatology* **49**, 809-820 (2009).
5. Sugimoto, M.A., Sousa, L.P., Pinho, V., Perretti, M. & Teixeira, M.M. Resolution of Inflammation: What Controls Its Onset? *Frontiers in immunology* **7**, 160 (2016).
6. Medzhitov, R. Origin and physiological roles of inflammation. *Nature* **454**, 428-435 (2008).
7. Dinarello, C.A., Simon, A. & van der Meer, J.W. Treating inflammation by blocking interleukin-1 in a broad spectrum of diseases. *Nature reviews. Drug discovery* **11**, 633-652 (2012).
8. Afonina, I.S., Zhong, Z., Karin, M. & Beyaert, R. Limiting inflammation-the negative regulation of NF-kappaB and the NLRP3 inflammasome. *Nature immunology* **18**, 861-869 (2017).
9. Szabo, G. & Csak, T. Inflammasomes in liver diseases. *Journal of hepatology* **57**, 642-654 (2012).
10. Strowig, T., Henao-Mejia, J., Elinav, E. & Flavell, R. Inflammasomes in health and disease. *Nature* **481**, 278-286 (2012).
11. Latz, E., Xiao, T.S. & Stutz, A. Activation and regulation of the inflammasomes. *Nature reviews. Immunology* **13**, 397-411 (2013).
12. Martinon, F., Mayor, A. & Tschopp, J. The inflammasomes: guardians of the body. *Annual review of immunology* **27**, 229-265 (2009).
13. Davis, B.K., Wen, H. & Ting, J.P. The inflammasome NLRs in immunity, inflammation, and associated diseases. *Annual review of immunology* **29**, 707-735 (2011).
14. Schroder, K., Zhou, R. & Tschopp, J. The NLRP3 inflammasome: a sensor for metabolic danger? *Science* **327**, 296-300 (2010).
15. Petrasek, J., *et al.* IL-1 receptor antagonist ameliorates inflammasome-dependent alcoholic steatohepatitis in mice. *The Journal of clinical investigation* **122**, 3476-3489 (2012).
16. Tilg, H., Moschen, A.R. & Szabo, G. Interleukin-1 and inflammasomes in alcoholic liver disease/acute alcoholic hepatitis and nonalcoholic fatty liver disease/nonalcoholic steatohepatitis. *Hepatology* **64**, 955-965 (2016).
17. Csak, T., *et al.* Fatty acid and endotoxin activate inflammasomes in mouse hepatocytes that release danger signals to stimulate immune cells. *Hepatology* **54**, 133-144 (2011).
18. Dixon, L.J., Flask, C.A., Papouchado, B.G., Feldstein, A.E. & Nagy, L.E. Caspase-1 as a central regulator of high fat diet-induced non-alcoholic steatohepatitis. *PloS one* **8**, e56100 (2013).
19. Wree, A., *et al.* NLRP3 inflammasome activation results in hepatocyte pyroptosis, liver inflammation, and fibrosis in mice. *Hepatology* **59**, 898-910 (2014).
20. Alegre, F., Pelegrin, P. & Feldstein, A.E. Inflammasomes in Liver Fibrosis. *Seminars in liver disease* **37**, 119-127 (2017).
21. Kazankov, K., *et al.* The role of macrophages in nonalcoholic fatty liver disease and nonalcoholic steatohepatitis. *Nature reviews. Gastroenterology & hepatology* **16**, 145-159 (2019).
22. Cartier, A. & Hla, T. Sphingosine 1-phosphate: Lipid signaling in pathology and therapy. *Science* **366**(2019).
23. Pappu, R., *et al.* Promotion of lymphocyte egress into blood and lymph by distinct sources of sphingosine-1-phosphate. *Science* **316**, 295-298 (2007).
24. Venkataraman, K., *et al.* Vascular endothelium as a contributor of plasma sphingosine 1-phosphate. *Circulation research* **102**, 669-676 (2008).
25. Mizugishi, K., *et al.* Essential role for sphingosine kinases in neural and vascular development. *Molecular and cellular biology* **25**, 11113-11121 (2005).
26. Rivera, J., Proia, R.L. & Olivera, A. The alliance of sphingosine-1-phosphate and its receptors in immunity. *Nature reviews. Immunology* **8**, 753-763 (2008).
27. Alvarez, S.E., *et al.* Sphingosine-1-phosphate is a missing cofactor for the E3 ubiquitin ligase TRAF2.

Nature **465**, 1084-1088 (2010).
28. Maceyka, M. & Spiegel, S. Sphingolipid metabolites in inflammatory disease. *Nature* **510**, 58-67 (2014).
29. Wang, F.*, et al.* Sphingosine-1-phosphate receptor-2 deficiency leads to inhibition of macrophage proinflammatory activities and atherosclerosis in apoE-deficient mice. *The Journal of clinical investigation* **120**, 3979-3995 (2010).
30. Lee, S.Y.*, et al.* Activation of sphingosine kinase 2 by endoplasmic reticulum stress ameliorates hepatic steatosis and insulin resistance in mice. *Hepatology* **62**, 135-146 (2015).
31. Hou, L.*, et al.* Macrophage Sphingosine 1-Phosphate Receptor 2 Blockade Attenuates Liver Inflammation and Fibrogenesis Triggered by NLRP3 Inflammasome. *Frontiers in immunology* **11**, 1149 (2020).
32. Liu, X.*, et al.* Essential roles of sphingosine 1-phosphate receptor types 1 and 3 in human hepatic stellate cells motility and activation. *Journal of cellular physiology* **226**, 2370-2377 (2011).
33. Yang, L.*, et al.* Sphingosine kinase/sphingosine 1-phosphate (S1P)/S1P receptor axis is involved in liver fibrosis-associated angiogenesis. *Journal of hepatology* **59**, 114-123 (2013).
34. Calabresi, P.A.*, et al.* Safety and efficacy of fingolimod in patients with relapsing-remitting multiple sclerosis (FREEDOMS II): a double-blind, randomised, placebo-controlled, phase 3 trial. *The Lancet. Neurology* **13**, 545-556 (2014).
35. Blaho, V.A. & Hla, T. An update on the biology of sphingosine 1-phosphate receptors. *Journal of lipid research* **55**, 1596-1608 (2014).
36. Liu, G.*, et al.* Targeting S1P1 receptor protects against murine immunological hepatic injury through myeloid-derived suppressor cells. *Journal of immunology* **192**, 3068-3079 (2014).
37. Yin, X.D., Jia, P.J., Pang, Y. & He, J.H. Protective effect of FTY720 on several markers of liver injury induced by concanavalin a in mice. *Current therapeutic research, clinical and experimental* **73**, 140-149 (2012).
38. Kaneko, T.*, et al.* Sphingosine-1-phosphate receptor agonists suppress concanavalin A-induced hepatic injury in mice. *Biochemical and biophysical research communications* **345**, 85-92 (2006).
39. Moro-Sibilot, L.*, et al.* Mouse and Human Liver Contain Immunoglobulin A-Secreting Cells Originating From Peyer's Patches and Directed Against Intestinal Antigens. *Gastroenterology* **151**, 311-323 (2016).
40. Mauer, A.S., Hirsova, P., Maiers, J.L., Shah, V.H. & Malhi, H. Inhibition of sphingosine 1-phosphate signaling ameliorates murine nonalcoholic steatohepatitis. *American journal of physiology. Gastrointestinal and liver physiology* **312**, G300-G313 (2017).
41. Enriquez-Marulanda, A.*, et al.* Cerebral toxoplasmosis in an MS patient receiving Fingolimod. *Multiple sclerosis and related disorders* **18**, 106-108 (2017).
42. Li, P.Z., Li, J.Z., Li, M., Gong, J.P. & He, K. An efficient method to isolate and culture mouse Kupffer cells. *Immunol Lett* **158**, 52-56 (2014).
43. Koh, E.H.*, et al.* Sphingomyelin synthase 1 mediates hepatocyte pyroptosis to trigger non-alcoholic steatohepatitis. *Gut* **70**, 1954-1964 (2021).
44. Choi, J.W.*, et al.* FTY720 (fingolimod) efficacy in an animal model of multiple sclerosis requires astrocyte sphingosine 1-phosphate receptor 1 (S1P1) modulation. *Proceedings of the National Academy of Sciences of the United States of America* **108**, 751-756 (2011).
45. Jang, J.E.*, et al.* Protective role of endogenous plasmalogens against hepatic steatosis and steatohepatitis in mice. *Hepatology* **66**, 416-431 (2017).
46. Farrell, G.*, et al.* Mouse Models of Nonalcoholic Steatohepatitis: Toward Optimization of Their Relevance to Human Nonalcoholic Steatohepatitis. *Hepatology* **69**, 2241-2257 (2019).
47. Matsumoto, M.*, et al.* An improved mouse model that rapidly develops fibrosis in non-alcoholic steatohepatitis. *International journal of experimental pathology* **94**, 93-103 (2013).
48. Schwabe, R.F., Tabas, I. & Pajvani, U.B. Mechanisms of Fibrosis Development in Nonalcoholic Steatohepatitis. *Gastroenterology* **158**, 1913-1928 (2020).
49. Mridha, A.R.*, et al.* NLRP3 inflammasome blockade reduces liver inflammation and fibrosis in experimental NASH in mice. *Journal of hepatology* **66**, 1037-1046 (2017).
50. Dillmann, C., Mora, J., Olesch, C., Brune, B. & Weigert, A. S1PR4 is required for plasmacytoid dendritic cell differentiation. *Biological chemistry* **396**, 775-782 (2015).
51. Schuster, C.*, et al.* S1PR4-dependent CCL2 production promotes macrophage recruitment in a murine psoriasis model. *European journal of immunology* **50**, 839-845 (2020).
52. He, Y., Hara, H. & Nunez, G. Mechanism and Regulation of NLRP3 Inflammasome Activation. *Trends in biochemical sciences* **41**, 1012-1021 (2016).
53. Gong, T., Yang, Y., Jin, T., Jiang, W. & Zhou, R. Orchestration of NLRP3 Inflammasome Activation by

Ion Fluxes. *Trends in immunology* **39**, 393-406 (2018).
54. Lee, G.S., *et al.* The calcium-sensing receptor regulates the NLRP3 inflammasome through Ca2+ and cAMP. *Nature* **492**, 123-127 (2012).
55. Yamazaki, Y., *et al.* Edg-6 as a putative sphingosine 1-phosphate receptor coupling to Ca(2+) signaling pathway. *Biochemical and biophysical research communications* **268**, 583-589 (2000).
56. Raffaello, A., Mammucari, C., Gherardi, G. & Rizzuto, R. Calcium at the Center of Cell Signaling: Interplay between Endoplasmic Reticulum, Mitochondria, and Lysosomes. *Trends in biochemical sciences* **41**, 1035-1049 (2016).
57. Chiang, C.Y., Veckman, V., Limmer, K. & David, M. Phospholipase Cgamma-2 and intracellular calcium are required for lipopolysaccharide-induced Toll-like receptor 4 (TLR4) endocytosis and interferon regulatory factor 3 (IRF3) activation. *The Journal of biological chemistry* **287**, 3704-3709 (2012).
58. Schappe, M.S., *et al.* Chanzyme TRPM7 Mediates the Ca(2+) Influx Essential for Lipopolysaccharide-Induced Toll-Like Receptor 4 Endocytosis and Macrophage Activation. *Immunity* **48**, 59-74 e55 (2018).
59. Rohrbach, T., Maceyka, M. & Spiegel, S. Sphingosine kinase and sphingosine-1-phosphate in liver pathobiology. *Critical reviews in biochemistry and molecular biology* **52**, 543-553 (2017).
60. Hanson, M.A., *et al.* Crystal structure of a lipid G protein-coupled receptor. *Science* **335**, 851-855 (2012).
61. Pham, T.C., *et al.* Molecular recognition in the sphingosine 1-phosphate receptor family. *Journal of molecular graphics & modelling* **26**, 1189-1201 (2008).
62. Oo, M.L., *et al.* Immunosuppressive and anti-angiogenic sphingosine 1-phosphate receptor-1 agonists induce ubiquitinylation and proteasomal degradation of the receptor. *The Journal of biological chemistry* **282**, 9082-9089 (2007).
63. Stepanovska, B. & Huwiler, A. Targeting the S1P receptor signaling pathways as a promising approach for treatment of autoimmune and inflammatory diseases. *Pharmacological research* **154**, 104170 (2020).
64. Dillmann, C., *et al.* S1PR4 Signaling Attenuates ILT 7 Internalization To Limit IFN-alpha Production by Human Plasmacytoid Dendritic Cells. *Journal of immunology* **196**, 1579-1590 (2016).
65. Seki, E. & Schwabe, R.F. Hepatic inflammation and fibrosis: functional links and key pathways. *Hepatology* **61**, 1066-1079 (2015).
66. Parthasarathy, G., Revelo, X. & Malhi, H. Pathogenesis of Nonalcoholic Steatohepatitis: An Overview. *Hepatology communications* **4**, 478-492 (2020).
67. Wree, A., *et al.* NLRP3 inflammasome driven liver injury and fibrosis: Roles of IL-17 and TNF in mice. *Hepatology* **67**, 736-749 (2018).
68. Kim, K.M., *et al.* Galpha12 overexpression induced by miR-16 dysregulation contributes to liver fibrosis by promoting autophagy in hepatic stellate cells. *Journal of hepatology* **68**, 493-504 (2018).
69. Younossi, Z., *et al.* Global Perspectives on Nonalcoholic Fatty Liver Disease and Nonalcoholic Steatohepatitis. *Hepatology* **69**, 2672-2682 (2019).
70. Geng, T., *et al.* SphK1 mediates hepatic inflammation in a mouse model of NASH induced by high saturated fat feeding and initiates proinflammatory signaling in hepatocytes. *Journal of lipid research* **56**, 2359-2371 (2015).
71. Olesch, C., *et al.* S1PR4 ablation reduces tumor growth and improves chemotherapy via CD8+ T cell expansion. *The Journal of clinical investigation* **130**, 5461-5476 (2020).

This dissertation is produced from 'Sphingosine 1-phosphate receptor 4 promotes nonalcoholic steatohepatitis by activating NLRP3 inflammasome' published online by CMGH (2021)

국문요약

비알코올성 지방간질환 (nonalcoholic fatty liver disease, NAFLD)은 단순지방간에서부터 시작하여 비알코올성 지방간염 (nonalcoholic steatohepatitis, NASH), 간경화 (cirrhosis), 간암 (hepatocellular carcinoma)으로 진행하며 최근 비만 및 이에 따른 인슐린 저항성과 더불어 유병율이 급증하고 있다. 이에 대한 많은 연구들이 이루어지고 있으나 아직까지 이에 대한 치료제는 없는 없는 상태이다.

NLRP3 면역복합체는 미생물의 침입과 세포 내 위험 신호를 감지하여 염증성 사이토카인인 interleukin-1β (IL-1β)와 interleukin-18 (IL-18)을 분비하여 염증반응을 일으킨다. 이는 대식세포 등 다양한 면역세포 뿐만 아니라 최근 비만, 당뇨병 등 대사 질환에서 비면역세포인 지방세포 등에서도 중요한 병인임이 밝혀졌으며, NLRP3 면역복합체의 활성화가 비알코올성 지방간염의 간 조직내 염증과 섬유증에도 크게 기여한다고 보고되었다. 특히 손상된 간세포로부터 방출되는 다양한 damage-associated molecular patterns이 간 조직 내 간세포 및 대식세포의 NLRP3 활성화에 기여한다고 알려져 있다.

Sphingosine-1-phosphate(S1P)는 ceramide로부터 만들어지는 sphingosine이 phosphorylation되어 생성되는 signaling molecule로서 생성된 S1P는 세포 밖으로 유출된 후 다른 세포의 세포막에 있는 S1P receptor (S1PR)를 자극함으로써 작용을 하는 것으로 알려져 있다.

본 연구에서는 S1PR의 isofom 중 S1PR4가 다양한 비알코올성 지방간염 동물모델에서 증가되었음을 확인하였다. 그리고 S1PR4를 유전적으로 제어한 생쥐 동물 모델에서는 NASH의 발달이 억제됨을 확인하였으며 S1PR4가 세포 내 칼슘 이온을 조절함으로써 대식세포에서 NLRP3 활성화에 중요한 역할을 한다는 것을 밝혀냈다. 게다가 S1PR4의 길항제인 SLB736을 합성하여 동물모델에 투여하고 간 세포 내 대식세포의 NLRP3 활성화가 억제되는 것을 확인했다. 이는 비알코올성 지방간염이 발병되는데 있어서 간 조직 내의 대식세포에서 S1PR4-NLRP3의 활성화가 중심적인 역할을 한다는 것을 보여주고 있으며 NLRP3 면역복합체의 활성을 억제하기 위한 S1PR4의 길항제 개발이 비알코올성 지방간염의 치료를 위한 새로운 전략이 될 수 있음을 보여준다.